Research Paper

GEOSPHERE

GEOSPHERE; v. 13, no. 1

doi:10.1130/GES01314.1

12 figures; 4 tables

CORRESPONDENCE: gonzales_d@fortlewis.edu

CITATION: Gonzales, D.A., and Lake, E.T., 2017, Geochemical constraints on mantle-melt sources for Oligocene to Pleistocene mafic rocks in the Four Corners region, USA: Geosphere, v. 13, no. 1, p. 201–226, doi:10.1130/GES01314.1.

Received 11 January 2016
Revision received 12 September 2016
Accepted 3 November 2016
Final version published online 27 January 2017

THE GEOLOGICAL SOCIETY OF AMERICA®

Geochemical constraints on mantle-melt sources for Oligocene to Pleistocene mafic rocks in the Four Corners region, USA

David A. Gonzales[1] **and Ethan T. Lake**[2]

[1]Department of Geosciences, Fort Lewis College, 1000 Rim Drive, Durango, Colorado 81301, USA
[2]Department of Geological Sciences, The University of Texas at San Antonio, 1 UTSA Circle, San Antonio, Texas 78249, USA

ABSTRACT

Small masses of intraplate mafic plutonic and volcanic rocks are exposed in the Navajo volcanic field (26–24 Ma), Dulce dike swarm (25–20 Ma), and western San Juan Mountains (7–0.6 Ma) along the eastern boundary of the Colorado Plateau. Geochemical and Sr-Nd isotopic data for these rocks were employed to assess the time-space variations in melt compositions and to investigate the contributions from different mantle and crustal sources during magma production.

Geochemical data signify that post–26 Ma mantle melts produced in the Four Corners region were heterogeneous in composition, dominantly alkaline, and distinguished by trace-element patterns with elevated LILE and LREE. These magmas were generated by melting of metasomatized subcontinental lithospheric mantle (SCLM) with minor contributions from a mantle source that produced melts with geochemical affinities of oceanic island basalts. Nd and Sr isotopic data reveal that some melts could have experienced minor contamination (<1%) with upper crust, whereas the Dulce magmas formed by contamination of mantle melts with up to 40% lower crust or melting of SCLM with low time-integrated Sm/Nd. Relative to minettes in the Navajo volcanic field, mafic rocks in the western San Juan Mountains have similar Nd and Sr isotopic compositions but are lower in some chemical values (Mg#, K_2O, Rb, Zr, La/Lu, La/Ta, and Th/Yb) and higher in others (Al_2O_3, Na_2O, and CaO). We postulate that these different chemical traits are evidence of heterogeneity in the lithospheric mantle. Voluminous magma production involving mantle melts from 35 to 26 Ma could have modified the chemistry of the lithospheric mantle beneath the western San Juan Mountains. Alternatively, this region may be underlain by SCLM with distinct chemical attributes imparted by subduction processes during Proterozoic arc accretion. Our work provides a snapshot of broader regional trends wherein heterogeneity in mantle reservoirs was a major contributor to the variable compositions of mafic alkaline rocks produced over the Colorado Plateau and adjacent Southern Rocky Mountains after 26 Ma.

INTRODUCTION

Intraplate mantle melts were emplaced along the eastern edge of the Colorado Plateau in the Four Corners region after 26 Ma, producing three distinct fields of ultra to medium potassic mafic rocks (Figs. 1 and 2; Table 1). This record of episodic mantle magmatism is concentrated in zones of incipient crustal extension (Gonzales et al., 2010; Gonzales, 2015) defined by northeast-trending faults and dikes that span the northern margins of the San Juan Basin (SJB on Fig. 1). Mantle magmatism in the Four Corners region is broadly linked to regional, latest Paleogene to Neogene extension that created the Rio Grande rift (Fig. 1) (e.g., Smith, 2004).

The three fields of mafic rocks in the Four Corners area were placed in the upper crust in relative close proximity from 26 to 20 Ma and 7 to 0.6 Ma (Figs. 1 and 2). These samplings of mantle magmas thus afford an opportunity to investigate compositions of melt sources over time and evaluate the factors that influenced magmatism during the shift from compressional to extensional regional tectonics. In this contribution, we present a comprehensive comparison of geochemical and isotopic (Sr and Nd) data (Tables 2 and 3) for the different groups of mafic rocks (Fig. 2). Each group is distinguished by major- and trace-element compositions that define discrete but diffuse fields on chemical plots. Amongst the different groups, there is a gradational shift in chemical compositions, but the Sr and Nd isotopic data for the majority of these rocks are similar with a few notable distinctions. We postulate that the compositional variation amongst the different groups was influenced primarily by heterogeneity in metasomatized mantle lithosphere with a Proterozoic ancestry. The chemical signatures inherited from the SCLM were possibly modified by variable amounts of contamination with lower and upper crust. This investigation provides further insight into mantle-source heterogeneity and magmatic processes that influenced compositional variations in Oligocene to Pleistocene mantle rocks on a broader regional scale (Fig. 2) (e.g., Alibert et al., 1986; Leat et al., 1988; Johnson and Thompson, 1991; Tingey et al., 1991; Gibson et al., 1992, 1993).

REGIONAL GEOLOGIC SETTING

Latest Mesozoic to Cenozoic magmatism on the Colorado Plateau and adjacent Southern Rocky Mountains (Fig. 1) is attributed to shallow subduction of the Farallon plate during the Laramide orogeny, followed by slab rollback and regional Neogene extension (e.g., Coney and Reynolds, 1977; Humphreys, 1995; Humphreys et al., 2003; Chapin et al., 2004; Smith, 2004; Farmer et al., 2008; Chapin, 2012). It is hypothesized that starting around 30 Ma astheno-

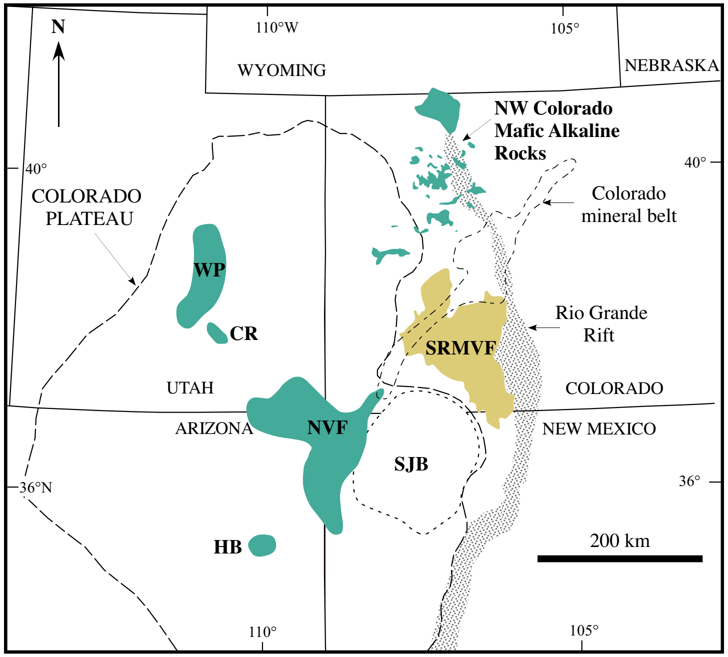

Figure 1. Latest Mesozoic to Cenozoic geologic and physiographic provinces in the Four Corners area: Navajo volcanic field (NVF); San Juan Basin (SJB); and Southern Rocky Mountains volcanic field (SRMVF; name applied by Lipman [2007] is synonymous with the San Juan volcanic field). Also shown are other major exposures of Oligocene to Pleistocene alkaline mafic rocks in the region that are of similar age and composition to post-26 Ma mafic rocks in the Four Corners region: (1) ca. 24, ca. 18, and ca. 7 Ma mafic dikes exposed on the Wasatch Plateau (WP) (Tingey et al., 1991); (2) 7–3 Ma mafic dikes in the Capitol Reef (CR) area (Gartner and Delaney, 1988); (3) 24–1 Ma mafic dikes, lava flows, and cinder cones in northwestern Colorado (Leat et at., 1988; Gibson et al., 1993); and (4) 5–2 Ma monchiquitte, nephelinite, and basanite lava flows and lava lakes that make up the Hopi Buttes (HB) (Alibert et al., 1986; Fitton et al., 1988). The stippled pattern shows the approximate extent of the Rio Grande rift.

spheric melts underplated and heated the metasomatized lithosphere (Schulze et al., 2015) at depths of 120–150 km beneath the eastern Colorado Plateau in response to the progressive rollback and delamination of the Farallon plate (e.g., Ehrenberg, 1979; Esperanca and Holloway, 1987; Roden et al., 1990; Smith et al., 1991; Tingey et al., 1991; Riter and Smith, 1996; Lee et al., 2001; Usui et al., 2002, 2003; Smith et al., 2004; Farmer et al., 2008). In the Four Corners region, melting of the lithospheric mantle produced alkaline mafic magmas that were emplaced in the upper crust in several pulses after 26 Ma (Fig. 2). The spatial distribution of these melts (Fig. 1) was broadly focused on northeast trends aligned with deep crustal fracture zones that formed by accretion and assembly of 1.8–1.75 Ga arc assemblages during the Yavapai orogeny (ca. 1.71 Ga) (e.g., Tweto and Sims, 1963; Tweto, 1980; Warner, 1980; Karlstrom et al., 2005). This is supported by seismic data from Gilbert et al. (2007) that documents distinct northeast variations in the crust-Moho structure on the eastern edge of the Colorado Plateau; they attribute these variations to crustal accretion and variable mantle metasomatism during the Proterozoic. Inheritance of 1.8–1.4 Ga zircons in 75–4 Ma felsic to intermediate plutonic rocks also reveals that Proterozoic basement contributed to the production of Cenozoic crustal magmas along this northeast-trending zone (Gonzales, 2015).

Geochemical and isotopic data for volcanic rocks in the Southern Rocky Mountains volcanic field (SRMVF) (Fig. 1) lend evidence that alkaline mantle melts contributed to the voluminous production of crustal magmas involved in volcanism from 32 to 25 Ma (e.g., Lipman et al., 1978; Slack and Lipman, 1979; Johnson, 1991; Riciputi et al., 1995; Lipman, 2007; Farmer et al., 2008; Lake, 2013; Lake and Farmer, 2015). Most of the mafic magmas remained at depth, but some were emplaced at shallow levels on the margins of the 29–27 Ma (e.g., Bove et al., 2001) San Juan–Silverton calderas (e.g., ca. 27 Ma Mount Sneffels–Stony Mountain gabbro-diorite stock; SN on Fig. 2). Continued emplacement of mantle melts within zones of minor extension (Gonzales, 2009, 2013, 2015; Gonzales et al., 2010) on the eastern edge of the Colorado Plateau (Fig. 1) likely contributed to elevated crustal geotherms that promoted small-volume crustal melting and production of post–26 Ma granitic to dioritic plutons in southwestern Colorado (Lipman et al., 1976; Lipman, 1989, 2007; Gonzales, 2015).

Although mafic magmas were intermittently emplaced at upper crustal levels across the Four Corners region after 26 Ma (Figs. 1 and 2), the greatest production was from 26 to 20 Ma (summarized in Gonzales, 2015). The ages and distribution of mafic rocks in the region define three distinct fields: (1) 26–24 Ma diatreme-dike complexes in the Navajo volcanic field (NVF); (2) 25–20 Ma dikes in the northern extension of the Dulce swarm; and (3) 7–0.6 Ma dikes and minor lava flows in the western San Juan Mountains (WSM) (Fig. 2). These Oligocene to Pleistocene mafic rocks are similar in age and composition to alkaline mafic dikes, lava flows, and cinder cones in northwestern Colorado (Leat et al., 1988; Gibson et al., 1993) and alkaline mafic dike swarms exposed on the Wasatch Plateau and Capitol Reef area in Utah (Gartner and Delaney, 1988; Tingey et al., 1991) (Fig. 1).

The Navajo volcanic field is distinguished by diatreme pipes and related maar craters, plugs, and shallow intrusive masses that span the east-central margin of the Colorado Plateau (Figs. 1 and 2) (Gregory, 1917; Williams, 1936; Appledorn and Wright, 1957; Akers et al., 1971; Naeser, 1971; Roden et al., 1979; Laughlin et al., 1986; Nowell, 1993; Gonzales et al., 2010). The latest Miocene alkaline mafic flows of the Hopi Buttes are exposed southwest of the Navajo volcanic field (e.g., Fitton et al., 1988; Alibert et al., 1986) (Fig. 1). Laughlin et al. (1986) and Nowell (1993) constrained the timing of NVF magmatism at 28–19 Ma, but more recent Ar-Ar analyses indicate that most of the magmatism was from 26 to 24 Ma (Gonzales et al., 2010; Nybo et al., 2011; Carrara, 2012; Nybo, 2014) in agreement with K-Ar ages of Roden et al. (1979) for minette at Buell Park. Nybo (2014) concluded that the ca. 9 Ma range in ages reported by Laughlin et al. (1986) and Nowell (1993) was probably a reflection of argon loss or excess argon in some of the samples analyzed.

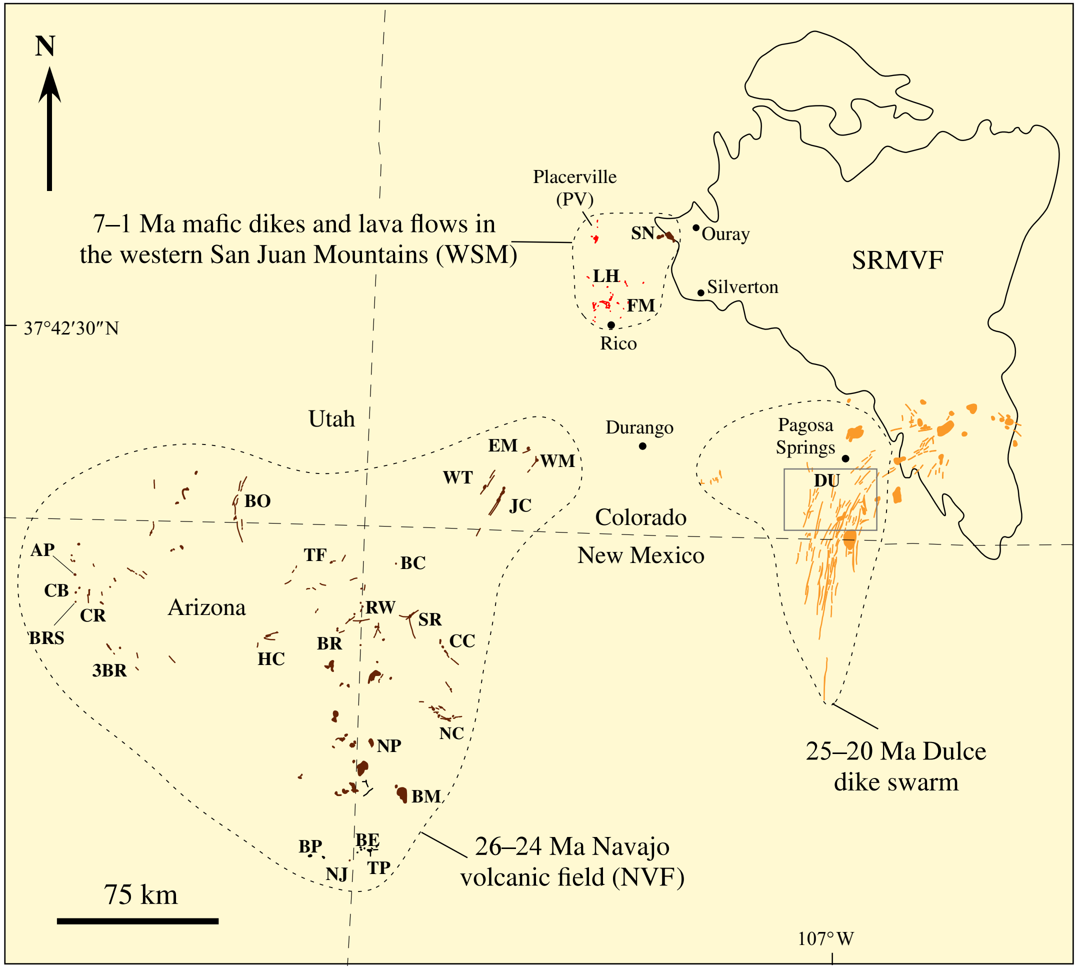

Figure 2. The general distribution of Oligocene to Pleistocene mafic plutonic and volcanic rocks that are exposed on the eastern margin of the Colorado Plateau and Southern Rocky Mountains in the Four Corners region. Sites in the Navajo volcanic field (NVF) are: Agathla Peak (AP), Beautiful Mountain (BM), Black Cone (BC), Black Rock Standing (BRS), Black Rock (BR), Boundary Butte (BO), Buell Park (BP), Cathedral Cliff (CC), Chaistla Butte (CB), Church Rock (CR), East Mancos Canyon (EM), Hasbidito Creek (HC), Johnson Canyon (JC), Narbona Pass (NP), Navajo (NJ), Newcomb (NC), Red Wash area (RW), Ship Rock (SR), The Beast (BE), Three Black Rocks (3BR), Todilto Park (TP), Twin Falls (TF), Weber Mountain (WM), and Wetherill Mesa (WT). Sites in the western San Juan Mountains (WSM) are: Flattop Mountain (FM), Lizard Head Pass (LH), Placerville (PV), and Mount Sneffels (SN). The box labeled DU in the field of the Dulce dike swarm outlines the area in which samples were collected. Sources that were used to compile this figure include Wood et al. (1948), Akers et al. (1971), Steven et al. (1974), Menzies et al. (1987), Condon (1990), and Lipman (2006).

Among the potassic rocks ($K_2O > Na_2O$) in the NVF (Figs. 1 and 2), minette is volumetrically the most abundant (minette as defined by Rock, 1977, 1991; Mitchell, 1995, 1997; Woolley et al., 1996; Steckeisen, 1979). The minettes are distinguished by phenocrysts of phlogopite + diopside ± olivine in groundmass dominated by phlogopite and sanidine (Table 2). Dikes of katungite (comparable to potassium-rich olivine melilitolite of Le Maitre et al., 1989) are exposed in a small swarm near Hasbidito Creek in Arizona (HC in Fig. 2). The katungites have phenocrysts of olivine and phlogopite in groundmass composed chiefly of phlogopite + melilite + perovskite + apatite ± clinopyroxene. Rocks with compositions that are transitional (Nowell, 1993) to minette and katungite are exposed in an east-west–trending dike swarm near Newcomb (NC on Fig. 2). These rocks have similar mineral assemblages to NVF minettes, although minor nepheline and melilite was identified by Nowell (1993) in some samples.

The 25–20 Ma Dulce dike swarm (Gonzales, 2015) crystallized from mantle melts that invaded a zone of minor extension on the northeast edge of the San Juan basin. The dike zone is roughly 100 km in length by ~30 km in width (Fig. 1). Farther to the northeast, this swarm melds with 20–26.5 Ma "dacite" dikes that radiate from the Platoro caldera complex in Colorado (Lipman, 2007; Lipman and Zimmerer, 2016). This relationship further hints at a magmatic connection (noted by Gonzales, 2015) of postcaldera crustal

TABLE 1. LOCATION INFORMATION AND GENERAL FEATURES OF OLIGOCENE TO PLEISTOCENE MAFIC ROCKS COLLECTED IN THE FOUR CORNERS REGION FOR THIS INVESTIGATION

Sample	Location §Longitude (°N)	§Latitude (°W)	Geologic feature	Geographic location (Fig. 1)	Classification on IUGS total alkali silica diagram
Navajo volcanic field (26 to 24 Ma) katungite†					
HC-1	109 20 42.9	36 38 13.8	Dike	Hasbidito Creek (HC)	Foidite
HC-3	109 22 33.0	36 37 41.9	Dike		
HC-4	109 22 33.0	36 37 41.0	Dike		
HC-5	109 24 28.0	36 36 51.0	Dike		
HC-7b	109 26 32.3	37 37 03.3	Dike		
Navajo volcanic field (26 to 24 Ma) transitional rocks††					
NC-1	108 37 20.6	36 21 16.1	Dike	Newcomb (NC)	Tephrite, foidite (NC3, NC-5)
NC-2	108 38 06.0	36 21 15.0	Dike		
NC-3	108 40 21.2	36 20 42.8	Dike		
NC-4	108 41 32.1	36 16 59.1	Dike		
NC-5	108 44 32.8	36 17 45.0	Dike		
NC-6	108 42 05.0	36 17 08.0	Dike		
Navajo volcanic field (26 to 24 Ma) minette†††					
Northern Arizona, Kayenta–Red Mesa area					
AP-1	110 13 24.3	36 49 33.0	Diatreme	Agathla Peak (AP)	Tephrite
BO-2a	109 33 41.8	37 02 22.8	Dike	Boundary Butte (BO)	Tephrite
BO-2b	109 33 41.8	37 02 22.8	Dike		Tephrite
BO-3	109 33 27.2	37 01 43.4	Dike		Tephrite
BRS-2	110 13 21.9	36 44 12.5	Plug	Black Rock Standing (BRS)	Basaltic trachyandesite
CB-1	110 12 24.0	36 46 50.3	Diatreme	Chaistla Butte (CB)	Basaltic trachyandesite
CR-1	110 07 05.2	36 43 59.7	Diatreme	Church Rock (CR)	Basaltic trachyandesite
6460-1	110 13 17.1	36 45 53.9	Diatreme	~1 mi SW of Chaistla Butte	Trachyandesite
3BR	109 57 58.8	36 30 43.5	Dike-plug	Three Black Rocks (3BR)	Isotope data only
Arizona-New Mexico border, Navajo–Buell Park area					
BE-1	109 01 32.3	35 54 32.2	Plug	The Beast (BE)	Trachyandesite
BP-1	109 04 55.4	35 53 47.2	Dike	Buell Park (BP)	Trachybasalt
NJ-1#	109 02 25.8	35 54 45.5	Plug	1 mile west of Navajo, New Mexico (NJ)	Trachyandesite
TP-4#	108 58 47.2	35 54 17.0	Plug-dike	Todilto Park (TP)	Basaltic trachyandesite
Northwestern New Mexico, Beautiful Mountain–Narbona Pass area					
BM-1	108 59 37.8	36 29 36.2	Sill	Beautiful Mountain (BM)	Basaltic trachyandesite
BM-2	108 59 36.8	36 29 37.4	Sill		Basaltic trachyandesite
NP-3#	108 52 26.7	36 05 16.8	Flow	Narbona Pass (NP)	Basaltic trachyandesite
Northwestern New Mexico and northeastern Arizona, Ship Rock–Twin Falls area					
BC-1	108 44 26.7	36 54 01.3	Pug	Black Cone (BC)	Trachyandesite
BR-1#	109 08 19.1	36 38 19.1	Plug	Black Rock (BR)	Basaltic trachyandesite
CC-1	108 42 21.2	36 36 18.8	Dike	Cathedral Cliff (CC)	Phonotephrite
RW-2	108 58 6.04	36 39 28.4	Dike	Red Wash (RW)	Foidite
RW-3	108 58 14.1	36 39 29.2	Plug		Tephrite
TF-1	109 07 03.0	36 52 25.8	Dike	Twin Falls (TF)	Phonotephrite
TF-2	109 07 03.3	36 52 26.2	Dike		Phonotephrite
SR-1	108 49 55.6	36 41 38.5	Plug	Ship Rock (SR)	Phonotephrite
SR-2	108 49 48.6	36 41 30.3	Plug		Phonotephrite
SR-6	108 49 47.5	36 38 52.1	Dike		Tephrite

(*continued*)

TABLE 1. LOCATION INFORMATION AND GENERAL FEATURES OF OLIGOCENE TO PLEISTOCENE MAFIC ROCKS COLLECTED IN THE FOUR CORNERS REGION FOR THIS INVESTIGATION (*continued*)

Sample	Location §Longitude (°N)	§Latitude (°W)	Geologic feature	Geographic location (Fig. 1)	Classification on IUGS total alkali silica diagram
Navajo volcanic field (26 to 24 Ma) transitional minette††† (*continued*)					
Southwestern Colorado, Mesa Verde area					
JC-3	108 27 35.6	37 05 57.9	Dike	Johnson Canyon (JC)	Phonotephrite
JC-4	108 27 36.3	37 05 56.4	Dike		Basaltic trachyandesite
JC-14	108 26 48.9	37 07 23.4	Dike		Phonotephrite
JC-MC139	108 27 22.3	37 06 02.3	Dike		Tephrite
WT-2	108°30′57.4	37 08 30.7	Dike	Wetherill Mesa (WT)	Trachyandesite
WT-11	108 31 15.3	37 08 17.9	Dike		Basaltic trachyandesite
WT-24	108 31 02.6	37 08 19.3	Dike		Trachyandesite
WT-26	108 30 57.5	37 08 30.6	Dike		Trachyandesite
L-11-EL-WM-01	108 21 13.9	37 16 04.5	Dike	Weber Mountain (WM)	Phonotephrite
L-11-EL-WM-03	108 20 54.2	37 16 24.1	Dike		Phonotephrite
L-11-EL-WM-05	108 20 53.4	37 16 26.4	Dike		Phonotephrite
WM1-04	108 20 53.9	37 16 27.9	Dike		Phonotephrite
WM1a-07	108 29 52.5	37 10 32.2	Dike		Basaltic trachyandesite
EM-1	108 21 47.6	37 15 28.2	Dike	East Mancos Canyon (EM)	Tephrite
Northern extent of Dulce dike swarm (25 to 20 Ma), kersantite*					
DU-1	108 37 20.6	37 02 08.7	Dike	Pagosa Springs (DU)	Tephrite
DU-2	108 38 06.0	37 03 19.9	Dike		Tephrite
DU-3	106 57 01.5	37 03 27.8	Dike		Trachybasalt
DU-5	106 59 30.9	37 03 36.6	Dike		Trachybasalt
DU-6	107 00 07.0	37 03 40.0	Dike		Basalt
DU-10	107 01 43.2	37 03 19.8	Dike		Trachybasalt
DU-16	106 57 37.7	37 06 52.1	Dike		Tephrite
Spessartite dikes**, western San Juan Mountains (7 to 4 Ma)					
L-10-EL-FM-01S	107 59 35.6	37 46 08.9	Dike	Flattop Mountain (FM)	Foidite
L-10-EL-FM-01C	107 59 35.6	37 46 08.9	Dike		Tephrite
L-10-EL-FM-03L	107 55 25.9	37 46 06.6	Dike		Tephrite
L-10-EL-FM-03R	107 55 25.9	37 46 06.6	Dike		Tephrite
L-11-EL-CM-06	107 57 15.9	37 49 27.7	Dike	Lizard Head (LH)	Basalt
L-11-EL-CM-07	107 57 32.4	37 50 01.4	Dike		Tephrite
L-11-EL-CM-08	107 57 41.7	37 50 05.0	Dike		Tephrite
Kersantite dikes***, western San Juan Mountains (7 to 4 Ma)					
L-10-EL-FM-02	107 59 26.4	37 46 10.85	Dike	Flattop Mountain (FM)	Tephrite
L-10-EL-BB-01	107 58 05.5	37 51 06.5	Dike	Lizard Head (LH)	Basalt
L-10-EL-CM-04L	107 57 24.5	37 49 46.2	Dike		Basalt
LH-7	107 57 24.9	37 50 02.9	Dike		Trachybasalt
LH-8	107 57 37.3	37 50 16.3	Dike		Basalt
LH-9	107 58 19.2	37 51 05.1	Dike		Basalt
LH-10a	107 57 28.4	37 50 05.3	Dike		Trachybasalt
LH-11	107 57 15.7	37 49 56.4	Dike		Trachybasalt
L-11-EL PV-01S	108 04 21.1	38 01 26.8	Dike	Placerville (PV)	Foidite
L-11-EL PV-01C	108 04 21.1	38 01 26.8	Dike		Foidite
PV-1	108 04 20.7	38 01 28.7	Dike		Tephrite

(*continued*)

TABLE 1. LOCATION INFORMATION AND GENERAL FEATURES OF OLIGOCENE TO PLEISTOCENE MAFIC ROCKS COLLECTED IN THE FOUR CORNERS REGION FOR THIS INVESTIGATION (*continued*)

Sample	Location §Longitude (°N)	§Latitude (°W)	Geologic feature	Geographic location (Fig. 1)	Classification on IUGS total alkali silica diagram
Olivine basalt**** lava flow, western San Juan Mountains (614 ka)					
SPM-1	108 04 44.4	37 58 15.1	Lava flow	Specie Mesa west of Placerville (PV)	Tephrite
SPM-2	108 04 20.1	37 58 16.8	Lava flow		

§Longitude and latitude coordinates are in degrees, minutes, and seconds.
†Katungite or olivine melilitotite as defined by Le Maitre et al. (1989) and Woolley et al. (1996): Porphyritic aphanitic with 1–8 mm phenocrysts of olivine and phlogopite in a groundmass composed chiefly of phlogopite, melilite, perovskite, and apatite ± clinopyroxene.
††Transitional rocks (nephelinite of Nowell, 1993): Porphyritic aphanitic with 1 mm to 5 mm phenocrysts of diopside and phlogopite in a groundmass dominated by phlogopite, sanidine, apatite, and iron oxide ± nepheline. Nowell (1993) reported olivine, melilite, and perovskite in some samples.
†††Minette: Microporphyritic to porphyritic aphanitic with <1 mm to 6 mm phenocrysts of diopside and phlogopite in a groundmass composed of variable proportions of phlogopite, sanidine, apatite, opaque minerals ± olivine (rare). Olivine-bearing samples that were analyzed are indicated by a pound symbol (#). Minor alteration of olivine to chlorite and serpentine was documented. The abundance of phlogopite, diopside, and sanidine in these rocks along with (K > Na) are criteria that define them as minette (e.g., Steckeisen, 1979; Mitchell, 1995, 1997; Woolley et al., 1996).
*Kersantite, Dulce dike swarm: Aphanitic to porphyritic aphanitic; <1 mm to 4 mm phenocrysts clinopyroxene, phlogopite ± rare hornblende in a very fine grained groundmass of phlogopite, calcic plagioclase, opaque minerals ± rare sanidine, and apatite. Stringers and blebs of calcite are present in some outcrops. The abundance of phlogopite, diopsidic augite, and calcic plagioclase in the rocks along with (K > Na) are criteria that define it as kersantite (e.g., Rock, 1977; Steckeisen, 1979; Mitchell, 1995, 1997; Woolley et al., 1996).
**Spessartite dikes, western San Juan Mountains: Porphyritic aphanitic with 0.5 mm to 2 mm phenocrysts or microphenocrysts of clinopyroxene and amphibole ± biotite set in a fine-grained groundmass of biotite, opaque minerals, and feldspar (mostly plagioclase). Some outcrops contain calcite nodules, and in a few samples there is minor secondary alteration of phenocrysts to chlorite. Due to dominance of pyroxene and amphibole phenocrysts in these rocks, together with groundmass assemblages rich in plagioclase, these rocks are classified as spessartite (Steckeisen, 1979; Mitchell, 1995, 1997; Woolley et al., 1996).
***Kersantite dikes, western San Juan Mountains: Porphyritic aphanitic with 0.5 mm to 2 mm phenocrysts or microphenocrysts of clinopyroxene ± biotite ± altered olivine in very fine grained groundmass containing biotite, clinopyroxene, feldspar, and opaque minerals. The feldspar forms distinct laths or felty masses and includes plagioclase ± sanidine (or orthoclase). In sample PV-1, poikilitic sanidine makes up a large proportion of the groundmass. Some samples show very minor alteration of augite, biotite, and olivine to chlorite, and small blebs of magmatic (?) calcite in the groundmass. These rocks are classified as kersantite because of the phenocrysts types and higher proportion (about 5:1) of plagioclase in the groundmass (e.g., Steckeisen, 1979; Mitchell 1995, 1997; and Woolley et al., 1996).
****Olivine basalt: porphyritic aphanitic with 1 mm to 3 mm phenocrysts of olivine and augite in an aphanitic groundmass composed chiefly of microlites of calcic plagioclase, opaque minerals, and glass. Parts of the flow are scoriaceous with numerous vesicles from 1 mm to 2 cm; some vesicles are filled with calcite. Other zones in the flow contain only a few percent vesicles ranging from 1 mm to 3 mm. Some outcrops have a conspicuous flow lamination.

melts and mantle magmas on the east margin of the Colorado Plateau. We collected samples (Tables 1 and 2) from dikes exposed in Colorado within the northern extent of the Dulce swarm (Fig. 2). These rocks are texturally similar to NVF minettes but differ slightly in mineralogy (Table 1). They have K_2O > Na_2O (0.12–1.36, Table 2), and contain abundant phenocrysts of diopsidic augite and phlogopite in fine-grained groundmass dominated by calcic plagioclase. On the basis of these characteristics (Tables 1 and 2), we classify the Dulce rocks as kersantite (after Rock, 1977; Mitchell, 1995, 1997; Woolley et al., 1996; Steckeisen, 1979).

A small number of 7–4 Ma (Gonzales, 2015) mafic dikes were emplaced in the western San Juan Mountains (Bush et al., 1959, 1960; Bromfield, 1967) in close association with late Miocene to Pliocene felsic to intermediate hypabyssal plutons (Lipman et al., 1976; Wareham, 1991; Cunningham et al., 1994; Wareham et al., 1998; Gonzales, 2015). These dikes are exposed in a north to northeast zone that extends for ~100 km (Fig. 1). They were classified into two types of "lamprophyres" on the basis of mineral composition and chemistry by Bromfield (1967). One group is herein classified as kersantite (Rock, 1977; Steckeisen, 1979; Mitchell, 1995, 1997; Woolley et al., 1996) because the rocks contain phenocrysts of diopsidic augite, biotite, and minor olivine in groundmass dominated by plagioclase and lesser amounts of sanidine or orthoclase (Table 1). A few rocks in this group (identified with PV in Table 2) are distinguished by poikilitic sanidine in the groundmass, which was also observed in some NVF minettes. The other group of WSM "lamprophyres" are characterized by 1–3 mm phenocrysts of clinopyroxene and green to brown amphibole set in fine-grained groundmass containing biotite, opaque minerals, and feldspar (dominated by plagioclase). The dominance of pyroxene + amphibole in these rocks, together with groundmass assemblages, define these rocks as spessartite (after Rock, 1977; Mitchell, 1995, 1997; Woolley et al., 1996; Steckeisen, 1979).

A basaltic lava flow exposed on Specie Mesa near Placerville represents the most recent product of mantle magmatism in the region (Fig. 2; Tables 1 and 2). The flow erupted along a series of north to northwest-trending normal faults, and on the basis of field relationships it was interpreted as Quaternary (Bush et al., 1960). A new $^{40}Ar/^{39}Ar$ whole-rock analysis constrains the age of the flow at 614 ± 5 ka (personal commun., M. Heizler, 2016, New Mexico Geochronology Research Laboratory).

TABLE 2. MAJOR- AND TRACE-ELEMENT DATA FOR SAMPLES OF OLIGOCENE TO PLEISTOCENE MAFIC ROCKS FROM THE FOUR CORNERS REGION (THIS STUDY)

		Major-element oxides (wt%)														Trace elements (ppm)																								
Sample number*	Rock type	SiO_2	TiO_2	Al_2O_3	Fe_2O_3	FeO	MnO	MgO	CaO	Na_2O	K_2O	P_2O_5	LOI	Total	K_2O/Na_2O	Cr	Ni	Y	Zr	Nb	Hf	Ta	Th	Ba	Rb	Sr	La	Ce	Pr	Nd	Sm	Eu	Gd	Tb	Dy	Ho	Er	Tm	Yb	Lu
Navajo volcanic field, Hasbidito Creek																																								
HC-1	Katungite	35.23	4.40	6.95	5.01	7.88	0.20	15.35	13.10	2.87	2.95	1.59	2.24	97.78	1.03	440	390	31.5	554	195	10.7	12.5	19.6	2032	91	1726	155.0	293	31.7	121	19.3	5.02	13.3	1.61	7.43	1.23	2.99	0.36	2.07	0.30
HC-3		34.92	4.58	5.75	6.34	6.07	0.18	16.46	11.74	1.24	1.77	1.33	8.75	99.13	1.43	520	450	24.5	454	172	9.0	12.5	17.3	1513	60	1428	134.0	254	27.4	104	17.0	4.30	11.3	1.36	6.02	0.98	2.30	0.26	1.49	0.21
HC-3		34.95	4.46	6.55	4.86	8.30	0.21	15.62	13.60	2.09	2.82	1.75	2.70	97.91	1.35	440	380	33.2	538	208	10.5	13.2	21.7	1867	85	1865	177.0	337	36.3	135	21.6	5.60	14.6	1.81	8.13	1.29	3.16	0.39	2.12	0.30
HC-5		34.67	4.54	6.98	5.44	8.03	0.21	14.21	14.33	2.20	2.88	1.93	3.22	98.64	1.31	390	310	36.3	584	217	11.5	13.3	21.6	2211	91	2032	187.0	354	38.1	141	22.5	5.85	15.5	1.92	8.77	1.43	3.41	0.41	2.29	0.32
HC-6		34.22	4.48	6.57	5.45	7.95	0.21	15.25	14.07	1.74	3.37	1.79	2.79	97.89	1.94	450	360	34.6	530	203	10.3	13.4	22.2	1917	91	1686	186.0	357	38.5	144	22.9	5.98	15.6	1.87	8.52	1.35	3.36	0.39	2.22	0.32
HC-7b		34.69	4.51	6.76	5.43	8.02	0.22	15.41	13.14	1.95	2.46	1.86	3.54	97.98	1.26	430	360	35.3	557	203	10.9	13.4	22.0	2028	83	2399	186.0	356	38.3	142	22.7	5.93	15.7	1.91	8.76	1.40	3.42	0.41	2.33	0.33
Navajo volcanic field, Newcomb area																																								
NC-1	Transitional rocks	44.48	2.53	9.07	4.37	4.5	0.13	11.72	11.03	2.20	3.36	1.37	3.20	97.96	1.53	470	310	29.1	384	69.2	7.8	4.9	50.0	2268	96	1274	164.0	303	35.0	139	24.7	5.66	15.8	1.69	7.02	1.12	2.53	0.29	1.58	0.22
NC-2		44.88	2.65	9.44	4.22	4.71	0.13	11.78	10.45	2.29	3.63	1.31	3.64	99.13	1.59	420	300	29.9	404	68.3	8.2	5.2	62.1	2597	98	1346	190.0	346	39.4	152	26.9	6.08	17.1	1.80	7.49	1.17	2.71	0.32	1.70	0.24
NC-3		40.96	3.36	8.35	5.67	4.71	0.15	11.96	11.88	2.09	2.28	1.16	5.50	98.07	1.09	420	270	26.1	457	133.0	9.2	10.0	27.8	6813	76	2760	134.0	255	28.7	112	19.7	4.89	13.3	1.54	6.50	1.01	2.38	0.27	1.48	0.22
NC-4		42.02	3.29	8.89	5.59	3.37	0.12	9.20	12.61	1.27	4.93	1.09	8.07	100.45	3.88	310	250	23.7	515	94.0	11.2	8.0	25.3	1731	115	1104	121.0	235	27.5	111	19.8	4.90	13.3	1.45	5.92	0.88	2.06	0.24	1.25	0.17
NC-5		34.85	3.36	8.96	5.56	3.72	0.55	6.98	15.55	0.62	4.92	1.10	12.86	99.03	7.94	330	300	25.8	515	94.9	11.4	8.2	26.4	1544	123	974	126.0	244	28.4	113	20.5	5.01	13.9	1.53	6.27	0.94	2.19	0.24	1.32	0.18
NC-6		43.55	3.35	8.63	5.06	4.14	0.12	11.68	10.21	1.06	5.01	1.17	5.79	99.77	4.73	450	330	26.3	497	69.4	12.2	5.2	22.2	1756	143	1022	124.0	248	30.7	98.4	20.4	5.30	14.5	1.59	6.58	0.88	1.94	0.22	1.19	0.14
Navajo volcanic field, Kayenta–Red Mesa area																																								
AP-1	Minette	47.02	1.98	9.78	4.26	4.71	0.15	10.20	10.30	2.38	4.35	1.10	1.78	98.01	1.83	330	260	30.6	421	88.1	8.0	5.7	48.8	2090	116	1507	171.0	314	34.9	134	23.3	5.45	14.9	1.67	7.10	1.10	2.58	0.32	1.87	0.26
BO-2a		43.44	2.93	8.85	5.80	4.43	0.18	13.02	10.81	1.44	3.23	1.07	4.80	100.01	2.24	590	380	27.1	426	123.0	10.1	6.4	29.9	1777	95	1060	143.0	257	29.8	107	18.1	4.41	11.9	1.34	6.19	0.95	2.11	0.27	1.64	0.24
BO-2b		41.19	2.91	8.72	5.65	4.50	0.18	12.74	10.51	1.42	3.10	1.10	5.40	97.41	2.18	560	330	26.6	374	96.4	8.9	6.1	30.0	1771	75	952	131.0	257	28.0	108	17.7	4.13	11.1	1.33	5.71	0.91	2.22	0.26	1.58	0.24
BO-3		43.47	3.35	7.77	3.99	5.57	0.14	13.05	10.03	2.96	2.06	1.17	4.28	97.84	0.70	410	370	24.1	478	121.0	10.0	9.1	48.8	2952	62	1463	173.0	316	34.7	129	21.1	4.92	13.0	1.43	6.08	0.91	2.12	0.25	1.33	0.18
BRS-2		50.02	1.74	10.24	3.63	4.06	0.13	9.32	9.13	2.20	5.10	0.93	1.68	98.18	2.32	320	220	24.8	380	65.8	8.0	4.8	59.4	2155	108	1463	159.0	286	32.0	122	20.9	4.73	13.0	1.44	6.09	0.93	2.22	0.28	1.56	0.22
CB-1		50.37	1.81	10.36	4.10	4.18	0.13	9.40	9.42	2.03	5.51	1.06	2.14	100.51	2.71	300	210	28.4	377	68.0	7.7	4.7	56.5	2245	130	1437	168.0	307	34.3	130	22.3	5.15	14.1	1.56	6.77	1.07	2.55	0.33	1.79	0.26
CR-1		52.83	1.28	11.00	5.12	2.23	0.12	8.06	7.98	2.59	5.05	0.86	1.93	99.05	1.95	330	240	26.8	374	48.9	9.1	2.4	59.2	2115	145	1380	153.0	262	32.5	118	20.2	4.64	12.2	1.29	5.63	0.85	1.98	0.26	1.57	0.23
6460-1		54.15	0.97	11.26	5.68	0.90	0.01	7.45	6.81	2.55	5.80	0.81	2.63	99.21	2.27	300	280	23.0	329	17.4	7.4	1.2	74.0	2417	144	1379	155.0	273	32.9	126	21.6	4.80	12.2	1.31	5.77	0.84	1.98	0.24	1.44	0.22
Navajo volcanic field, Navajo–Buell Park area																																								
BE-1	Minette	54.41	1.54	11.02	2.98	3.56	0.11	7.81	7.56	2.11	7.18	1.11	1.09	100.48	3.40	240	190	29.2	466	44.1	9.6	2.9	49.6	2795	185	1382	179.0	326	37.3	144	25.6	5.62	16.0	1.72	7.14	1.07	2.50	0.30	1.70	0.23
BP-1		49.21	2.19	9.78	5.15	3.20	0.12	10.50	8.97	1.65	5.21	1.04	3.53	100.55	3.16	350	270	23.6	436	73.3	8.6	5.1	22.6	2406	96	1363	117.0	219	25.1	98.9	17.8	4.26	11.9	1.32	5.82	0.87	1.90	0.23	1.33	0.19
NJ-1		55.07	1.43	11.09	2.92	3.35	0.09	7.45	7.28	1.99	7.32	1.00	1.27	100.26	3.68	230	190	30.5	483	36.6	9.9	2.5	57.8	2920	195	1355	190.0	346	39.9	155	27.2	5.90	16.8	1.81	7.46	1.11	2.61	0.31	1.72	0.24
TP-4		51.19	1.89	8.54	3.28	4.10	0.12	11.39	8.42	1.72	5.12	1.07	1.48	98.32	2.98	530	410	24.4	327	54.5	6.7	3.4	28.7	2412	139	1286	132.0	244	29.7	116	20.4	4.87	12.4	1.41	6.41	0.92	2.04	0.24	1.49	0.22
Navajo volcanic field, Beautiful Mountain–Narbona Pass area																																								
BM-1	Minette	50.89	1.94	10.36	3.98	3.97	0.13	8.51	9.09	2.20	5.43	0.86	1.74	99.10	2.47	290	200	23.7	385	59.7	8	4.3	36.5	2339	151	1375	124.0	224	25.1	95.5	16.2	3.76	10.00	1.19	5.33	0.86	2.13	0.28	1.64	0.23
BM-2		53.22	1.65	10.63	5.19	2.07	0.12	7.48	7.71	2.35	5.83	0.83	1.56	98.64	2.48	270	180	22.4	363	43.8	7.6	3.4	38.5	2316	171	1154	121.0	217	24.5	92.5	15.7	3.62	10.20	1.14	5.09	0.81	2.06	0.27	1.54	0.22
NP-3		52.11	2.13	10.24	3.96	3.64	0.12	9.60	7.64	1.87	5.91	0.75	1.33	99.30	3.16	370	270	18.3	427	58.9	9.3	4.7	49.5	2188	174	1272	125.0	225	24.5	92.0	14.8	3.45	9.30	1.06	4.57	0.73	1.71	0.21	1.23	0.18
Navajo volcanic field, Ship Rock–Twin Falls area																																								
BC-1	Minette	53.90	2.14	10.73	4.16	3.01	0.09	5.9	6.72	1.99	7.54	1.36	0.98	98.52	3.79	190	140	35.4	488	61.6	12.8	2.8	53.5	3978	245	1734	235.0	404	49.2	172.0	28.0	6.40	16.40	1.83	7.91	1.15	2.41	0.29	1.68	0.24
BR-1		51.23	2.04	10.5	3.04	4.66	0.12	8.99	7.85	1.94	5.5	0.72	2.21	98.80	2.84	340	230	21.7	405	61.4	8.4	4.4	34.5	1864	140	1039	105.0	191	20.9	78.8	13.1	3.14	8.82	1.03	4.78	0.81	2.08	0.27	1.60	0.23
CC-1		48.63	1.62	10.97	4.28	2.83	0.07	5.78	9.8	1.83	6.33	0.87	5.79	98.80	3.46	320	230	22.9	459	52.5	11.3	2.6	27.6	2003	207	1023	131.0	240	28.2	101.0	16.9	3.93	10.40	1.15	5.03	0.76	1.78	0.22	1.28	0.18
RW-2		39.04	3.77	6.8	6.83	4.53	0.17	16.52	11.43	0.83	1.61	1.33	7.15	100.01	1.94	850	530	25.5	393	101.0	9.9	7.0	21.3	1741	64	1189	118.0	231	27.4	85.5	15.6	4.26	11.60	1.32	5.97	0.93	2.20	0.27	1.39	0.17
RW-3		42.80	2.13	9.08	5.86	3.68	0.13	14.24	9.6	0.97	2.78	1.46	7.6	100.33	2.87	470	340	31.1	380	67.8	9.2	4.2	24.5	1989	78	929	139.0	272	33.6	109.0	21.6	5.76	16.10	1.78	7.62	1.12	2.60	0.31	1.71	0.20
TF-1		51.11	2.11	10.44	4.03	2.79	0.14	7.39	8.38	2.33	6.36	0.94	3.31	99.33	2.73	210	140	31.8	446	53.2	11.7	3.7	85.1	2979	158	1483	223.0	371	42.7	143.0	23.0	4.93	13.40	1.48	6.45	1.04	2.60	0.33	1.97	0.29
TF-2		51.50	2.08	10.6	4.03	3.1	0.12	7.1	7.91	2.07	6.43	0.93	2.95	98.82	3.11	230	140	27.5	414	51.8	9.9	3.4	87.6	2977	153	1398	189.0	343	35.7	133.0	21.0	4.29	12.20	1.31	5.68	0.91	2.42	0.28	1.78	0.27
SR-1		52.31	1.76	11.38	4.12	2.69	0.08	5.55	7.63	2.26	7.05	1.01	2.51	98.35	3.12	150	130	27.5	478	47.6	10.3	3.7	49.4	2754	202	1287	177.0	318	35.7	133.0	22.4	5.01	13.80	1.51	6.53	1.00	2.30	0.29	1.76	0.26
SR-2		51.32	1.99	10.77	4.16	3.25	0.09	7.88	7.24	1.81	6.46	1.01	2.14	98.12	3.57	240	200	26.2	448	52.5	9.5	4.0	46.1	2740	180	1295	165.0	293	32.4	122.0	20.6	4.68	12.90	1.44	6.24	0.98	2.37	0.30	1.71	0.26
SR-6		48.53	1.68	10.95	5.19	1.7	0.08	8.33	6.62	1.9	5.34	0.89	8.12	99.33	2.81	320	180	25.2	341	36.8	8.8	2.5	38.3	2312	128	1204	133.0	250	27.8	106.0	17.2	3.62	10.90	1.22	5.43	0.87	2.27	0.29	1.70	0.26

(*continued*)

TABLE 2. MAJOR- AND TRACE-ELEMENT DATA FOR SAMPLES OF OLIGOCENE TO PLEISTOCENE MAFIC ROCKS FROM THE FOUR CORNERS REGION (THIS STUDY) (*continued*)

		Major-element oxides (wt%)														Trace elements (ppm)																								
Sample number*	Rock type	SiO_2	TiO_2	Al_2O_3	Fe_2O_3	FeO	MnO	MgO	CaO	Na_2O	K_2O	P_2O_5	LOI	Total	K_2O/Na_2O	Cr	Ni	Y	Zr	Nb	Hf	Ta	Th	Ba	Rb	Sr	La	Ce	Pr	Nd	Sm	Eu	Gd	Tb	Dy	Ho	Er	Tm	Yb	Lu
Navajo volcanic field, Mesa Verde area																																								
JC-3	Minette	50.33	1.56	10.48	3.86	3.43	0.14	8.50	8.29	1.46	7.06	1.10	2.91	99.12	4.84	310	220	29.5	426	48.5	11.3	3.6	39.6	2102	199	1073	119.0	243	26.8	102.0	20.9	5.12	14.3	1.59	6.34	1.01	2.40	0.30	1.68	0.22
JC-4		49.81	1.52	9.44	3.91	3.23	0.13	9.37	9.75	1.42	5.60	0.98	3.33	98.49	3.94	410	330	25.8	366	64.6	9.7	3.4	32.3	1841	167	1003	119.0	222	26.6	97.5	19.9	4.95	15.3	1.66	6.59	0.98	2.39	0.29	1.66	0.22
JC-14		50.44	1.95	10.74	5.20	2.99	0.14	7.75	8.57	1.53	6.29	0.84	2.01	98.45	4.11	300	210	31.0	507	100.0	11.6	4.5	31.3	1665	162	766	146.0	250	29.9	106.0	18.0	4.41	11.6	1.40	6.57	1.03	2.45	0.33	2.00	0.29
JC-MC139		41.36	2.23	10.73	3.16	4.84	0.13	6.13	10.90	1.14	5.00	0.98	12.20	98.80	4.39	340	320	33.1	487	75.6	12.4	4.9	31.0	1821	130	1438	149.0	285	33.2	102.0	19.4	5.12	14.5	1.67	7.69	1.17	2.86	0.39	2.22	0.26
WT-2		55.69	1.10	10.49	3.76	1.90	0.09	8.51	6.13	1.69	6.31	0.74	2.62	99.03	3.73	370	370	21.5	347	26.0	10.3	1.4	54.3	2241	173	1032	143.0	260	30.0	99.3	19.4	4.51	13.7	1.30	5.03	0.75	1.88	0.24	1.35	0.19
WT-11		52.67	0.93	10.45	1.73	2.89	0.07	5.28	7.30	1.96	6.58	0.64	8.19	98.69	3.36	320	230	21.1	411	15.0	10.4	1.1	46.6	2102	194	969	124.0	228	29.1	91.4	16.0	3.87	9.7	0.97	4.36	0.70	1.69	0.21	1.11	0.14
WT-24		54.89	1.21	10.79	2.87	2.84	0.09	7.18	6.06	1.89	6.41	0.75	3.95	98.93	3.39	330	230	21.7	395	24.5	10.7	1.8	45.7	2287	181	933	131.0	240	28.7	89.7	16.5	3.94	11.4	1.21	5.29	0.82	1.96	0.26	1.41	0.19
WT-26		54.85	1.09	11.04	3.47	2.28	0.07	8.12	5.03	1.57	6.99	0.74	3.37	98.62	4.45	390	310	24.0	428	16.2	10.6	1.2	54.5	2354	185	1003	141.0	253	32.3	101.0	18.2	4.22	11.1	1.10	4.84	0.74	1.85	0.24	1.31	0.17
L-11-EL-WM-01		47.90	1.92	10.30	4.13	3.60	0.12	9.02	9.05	2.10	5.58	1.03	2.28	97.03	2.66	320	233	32.5	362	63.0	10.0	3.4	34.6	2220	158	1210	139.0	265	32.7	119.0	22.4	5.40	15.4	1.74	7.28	1.11	2.70	0.33	2.00	0.27
L-11-EL-WM-03		48.80	1.90	10.60	4.19	3.70	0.16	8.52	8.98	2.10	5.80	0.97	1.09	96.81	2.76	310	227	32.4	355	61.0	9.0	3.2	32.7	2130	159	1130	131.0	250	31.3	114.0	21.1	4.97	14.5	1.59	7.19	1.15	2.67	0.34	2.10	0.31
L-11-EL-WM-05		50.40	1.81	11.00	4.53	3.20	0.13	8.43	9.04	2.40	5.56	0.89	1.05	98.45	2.32	300	212	30.7	324	56.0	9.0	3.0	29.4	1940	142	1050	116.0	222	27.0	99.8	18.7	4.39	13.5	1.38	6.41	1.10	2.67	0.32	2.00	0.33
WM1-04		51.23	1.37	10.27	3.38	3.59	0.12	9.43	7.92	2.28	6.24	0.98	1.41	98.22	2.74	400	290	28.7	407	40.9	10.5	3.0	49.4	2112	184	1219	134.0	261	28.1	104.0	21.3	5.13	14.7	1.61	6.25	0.93	2.26	0.29	1.56	0.21
WM1a-07		53.17	0.93	10.28	1.27	3.13	0.07	5.97	6.73	1.86	6.63	0.65	7.92	98.61	3.56	290	220	19.3	372	16.8	10.2	1.3	52.8	2065	190	989	116.0	220	23.4	80.9	16.0	3.69	10.6	1.06	4.11	0.63	1.53	0.19	1.08	0.15
EM-1		47.38	1.41	10.34	3.63	3.74	0.07	6.03	9.49	1.59	4.76	0.90	9.39	98.73	2.99	400	290	27.0	410	56.3	10.1	2.6	44.1	1571	145	1155	143.0	246	30.8	112.0	19.4	4.46	12.0	1.34	5.77	0.87	1.94	0.25	1.46	0.21
Northern extent of Dulce dike swarm																																								
DU-1	Kersantite	47.00	1.87	16.55	6.37	4.51	0.20	5.64	5.26	5.07	0.62	0.71	4.20	98.00	0.12	30	80	21.0	192	16.7	4.6	0.9	1.8	1111	12	1251	41.8	89	11.2	38.5	7.5	2.19	6.41	0.85	4.40	0.76	1.99	0.26	1.49	0.20
DU-2		41.46	1.99	12.79	4.51	6.01	0.44	7.94	9.86	3.43	0.53	0.58	8.54	101.30	0.15	430	190	21.6	186	33.6	5.5	3.0	4.9	655	11	576	38.9	83	10.4	36.2	7.4	2.21	6.49	0.88	4.47	0.78	2.00	0.27	1.67	0.24
DU-3		50.49	1.69	12.18	3.91	4.56	0.10	8.44	7.00	2.42	3.28	0.56	3.78	98.14	1.36	580	100	21.6	226	14.6	6.1	0.6	4.1	479	205	602	39.7	92	11.9	48.0	9.4	2.55	7.22	0.93	4.44	0.75	1.89	0.26	1.62	0.24
DU-5		47.52	2.19	13.25	5.37	4.60	0.11	4.50	9.03	3.37	2.32	1.04	5.08	99.38	0.69	170	70	19.5	217	29.6	5.4	1.1	3.0	1625	33	1517	65.2	139	16.9	64.5	11.0	3.00	7.57	0.90	4.23	0.69	1.62	0.21	1.31	0.20
DU-6		47.86	1.80	13.02	5.58	3.72	0.09	4.51	8.05	3.54	1.00	0.87	7.71	97.75	0.28	280	80	18.0	222	27.1	5.4	1.0	2.8	4727	19	1279	59.3	127	15.1	57.1	9.6	2.41	6.34	0.77	3.71	0.61	1.50	0.20	1.26	0.19
DU-10		47.74	1.89	13.24	5.34	4.50	0.13	5.06	8.13	3.20	2.32	0.91	4.59	97.05	0.73	160	40	22.7	214	26.0	5.1	0.9	3.0	2263	34	1705	70.4	149	18.1	69.1	12.0	3.10	7.87	0.96	4.57	0.75	1.80	0.24	1.48	0.22
DU-16		43.16	2.04	13.65	4.50	5.04	0.12	5.04	9.15	3.11	2.65	0.90	9.00	98.36	0.85	130	70	22.4	260	34.7	5.9	2.3	3.4	1739	55	1305	51.8	112	14.3	57.9	10.4	2.92	7.70	0.97	4.73	0.84	2.19	0.29	1.72	0.26
Mafic dikes, western San Juan Mountains																																								
L-10-EL-FM-01S	Spessartite	36.1	2.21	11.80	4.88	4.80	0.17	3.97	12.6	0.6	3.95	0.95	14.30	96.33	6.58	420	214	28.1	229	74	5.0	3.9	12.3	1480	171	790	79.3	158	18.6	71.2	11.9	3.45	9.01	1.15	6.07	1.16	2.80	0.36	2.20	0.37
L-10-EL-FM-01C		41.5	2.15	11.00	4.50	5.50	0.12	8.04	12.5	0.9	3.03	0.92	5.38	95.54	3.37	380	168	24.1	219	71	5.0	3.7	12.2	2040	71	1180	75.6	147	17.1	66.8	11.0	2.86	8.14	1.04	5.28	1.00	2.30	0.33	1.90	0.24
L-10-EL-FM-03L		43.5	1.16	14.00	3.40	4.10	0.1	5.52	10.5	2.8	3.56	1.07	6.72	96.43	1.27	220	106	18.2	160	30	4.0	1.4	10.8	2160	72	1520	60.8	130	16.0	63.9	9.8	2.48	6.37	0.79	3.71	0.67	1.74	0.28	1.60	0.23
L-10-EL-FM-03R		47.1	1.19	15.00	3.66	4.00	0.11	7.01	6.42	2.3	4.42	1.16	8.02	100.39	1.92	170	87	18.6	170	33	4.0	1.5	11.8	1880	81	510	63.1	133	16.4	64.1	9.9	2.60	6.35	0.81	3.88	0.73	1.72	0.29	1.70	0.25
L-11-EL-CM-06		50.6	0.83	15.50	0.85	5.70	0.13	2.85	6.82	3.4	1.24	0.33	7.36	95.61	0.36	10	B.D.	25.1	141	12	4.0	B.D.	5.1	326	28	509	30.5	62	7.9	30.6	6.0	1.88	5.71	0.80	4.50	0.90	2.49	0.42	2.60	0.39
L-11-EL-CM-07		45.2	2.11	13.20	5.16	3.70	0.13	7.42	9.77	2.8	2.54	0.88	4.24	97.15	0.91	280	89	25.6	279	61	7.0	3.2	13.7	1860	40	1160	81.8	160	19.0	68.5	12.4	3.08	8.88	1.09	5.64	0.92	2.37	0.29	1.90	0.30
L-11-EL-CM-08		45.2	2.13	13.40	3.93	4.80	0.13	7.15	10.5	2.9	2.49	0.9	3.57	97.10	0.86	260	85	26.9	288	64	6.0	3.3	13.5	1670	41	1030	84.0	163	19.3	70.5	12.0	3.19	8.89	1.07	5.42	0.89	2.18	0.32	1.90	0.25
Mafic dikes, western San Juan Mountains																																								
L-10-EL-FM-02	Kersantite	42.10	2.43	11.70	5.10	5.50	0.14	9.83	12.30	1.00	2.82	0.97	3.59	97.48	2.82	340	136	25.7	222	73.0	5.0	3.9	12.6	1910	57	1410	78.3	155	18.3	71.0	12.0	3.28	9.22	1.21	5.81	1.02	2.52	0.34	2.20	0.29
L-10-EL-BB-01		47.00	1.94	12.40	4.13	4.50	0.17	7.22	11.00	2.50	2.36	0.79	4.15	98.16	0.94	390	139	22.5	254	55.0	6.0	2.8	11.4	1720	38	1160	73.5	144	16.9	65.4	10.8	2.86	7.61	1.00	4.80	0.90	2.17	0.31	1.90	0.28
L-10-EL-CM-04L		46.00	2.08	12.60	5.31	4.10	0.12	7.85	7.86	2.40	2.39	0.87	4.22	99.79	1.00	320	106	23.3	287	60.0	7.0	2.9	13.0	1780	39	1170	82.9	162	18.6	72.0	11.8	3.02	8.2	1.04	5.18	0.94	2.45	0.32	1.90	0.25
LH-7		46.88	2.05	12.73	6.39	3.75	0.14	7.08	9.37	2.67	2.44	0.87	4.35	98.72	0.91	210	B.D.	22.1	251	55.1	6.8	3.9	11.8	2044	35	1167	82.8	164	20.3	66.7	11.9	3.27	6.82	1.02	5.32	0.93	2.43	0.32	1.97	0.27
LH-8		47.16	2.08	12.78	3.19	4.57	0.12	6.82	11.58	2.46	2.20	0.92	4.75	98.63	0.89	250	B.D.	22.1	265	55.5	7.0	3.9	11.3	2057	32	1197	79.0	157	19.2	62.9	11.6	3.19	6.77	0.98	5.16	0.89	2.37	0.32	1.98	0.27
LH-9		46.69	2.01	12.17	4.99	3.89	0.15	7.22	11.59	2.26	2.29	0.87	4.91	99.04	1.01	390	B.D.	21.1	235	51.2	6.4	3.7	10.4	1782	31	1040	71.7	144	18.0	58.5	11.0	3.07	6.62	0.96	4.97	0.87	2.30	0.32	1.94	0.26
LH-10		49.02	2.08	12.92	5.26	3.66	0.20	6.75	10.05	3.06	2.47	0.90	2.39	98.76	0.81	250	B.D.	24.1	267	53.8	7.5	3.9	11.7	2026	33	1167	88.6	171	21.5	68.4	12.6	3.49	7.58	1.11	5.81	1.03	2.69	0.36	2.15	0.29
LH-11		47.44	2.00	12.38	5.77	3.48	0.14	8.00	9.32	2.51	2.38	0.91	5.18	99.51	0.95	240	B.D.	23.8	271	55.5	7.6	3.9	12.2	2173	35	1102	87.5	171	21.7	70.5	13.1	3.6	7.83	1.10	5.85	1.01	2.65	0.35	2.03	0.27
L-11-EL-PV-01S		39.40	2.89	11.20	4.88	5.60	0.17	9.91	12.10	2.10	2.34	1.02	4.72	96.33	1.11	450	225	26.4	271	98.0	7.0	5.4	9.7	1740	65	1270	77.7	153	18.0	66.5	12.7	3.36	9.78	1.16	5.49	0.97	2.28	0.31	1.70	0.24
L-11-EL-PV-01C		40.60	3.00	11.60	5.18	5.60	0.15	10.40	12.10	2.10	2.28	1.03	4.15	98.19	1.09	430	200	26.5	276	99.0	6.0	5.6	9.7	1950	73	1420	76.1	151	17.8	66.5	12.0	3.48	9.75	1.21	5.70	0.95	2.23	0.31	1.70	0.30
PV-1		41.86	2.78	11.59	4.64	5.91	0.12	9.88	11.63	1.68	2.35	1.11	4.35	97.90	1.40	380	190	26.4	319	123.0	6.6	6.3	9.8	2270	77	2047	83.1	159	17.6	65.8	11.5	3.22	8.54	1.10	5.47	0.92	2.24	0.29	1.76	0.26
Specie Mesa flow, western San Juan Mountains																																								
SPM-1	Olivine-pyroxene basalt	45.72	2.59	15.11	3.23	7.40	0.17	6.38	10.60	3.57	2.21	1.07	1.15	99.20	0.62	70	70	24.4	248	68.8	5.5	4.4	9.9	1879	39	1356	69.5	138	16.6	64.7	11.8	3.26	7.88	1.03	5.20	0.92	2.31	0.31	1.82	0.28
SPM-2		46.17	2.58	15.28	2.15	8.40	0.17	6.53	10.85	3.80	2.62	0.99	–0.08	99.46	0.69	70	70	24.1	243	67.9	5.7	4.4	9.9	1790	48	1324	69.5	139	16.6	64.9	11.5	3.37	8.06	1.04	5.26	0.87	2.24	0.30	1.86	0.29

*Locations of samples are shown on Figure 2 and listed in Table 1.
B.D.—Concentrations are below detection limits.

TABLE 3. STRONTIUM AND NEODYMIUM ISOTOPIC DATA FOR POST-26 Ma MAFIC ROCKS FROM THE FOUR CORNERS AREA (THIS STUDY)

Sample number	[Rb]*	[Sr]*	$^{87}Sr/^{86}Sr_{(m)}$	$^{87}Sr/^{86}Sr_{(i)}$	[Sm]*	[Nd]*	$^{143}Nd/^{144}Nd_{(m)}$	$\varepsilon_{Nd(t)}$[§]
Navajo volcanic field katungite (26–24 Ma)								
HC-1	84.8	1669.9	0.703985 ± 7	0.70393	19.9	121	0.512715 ± 12	1.83
HC-4	76	1832	0.704017 ± 8	0.70397	22.3	143.2	0.512714 ± 13	1.81
HC-6	N.D.	N.D.	N.D.	N.D.	22.9	148.1	0.512688 ± 13	1.3
HC-7b	75.1	2365	0.705230 ± 9	0.7052	23.5	151	0.512725 ± 9	2.02
Navajo volcanic field transitional rocks (26–24 Ma)								
NC-1	86.5	1253	0.706078 ± 14	0.70601	25.5	147.4	0.512573 ± 9	–0.97
NC-2	89.1	1297.2	0.706046 ± 8	0.70616	27.6	162.7	0.512569 ± 8	–1.05
Navajo volcanic field minette, northern Arizona, Kayenta–Red Mesa area (26–24 Ma)								
AP-1	103.9	1471.5	0.705355 ± 13	0.70528	24.2	144.1	0.512571 ± 15	–1
BO-2	N.D.	N.D.	N.D.	N.D.	17.5	105.5	0.512686 ± 11	1.3
BRS-2	N.D.	N.D.	N.D.	N.D.	21.4	124.9	0.512636 ± 12	0.26
CR-1	119.8	1345.3	0.706248 ± 9	0.70616	20.2	119.4	0.512648 ± 13	0.49
Navajo volcanic field minette, Arizona–New Mexico Border, Navajo–Buell Park area (26–24 Ma)								
BE-1	173.7	1288.4	0.706829 ± 9	0.70669	26.8	157.2	0.512538 ± 8	–1.65
Navajo volcanic field minette, northwestern New Mexico, Beautiful Mountain–Narbona Pass area (26–24 Ma)								
BM-1	N.D.	N.D.	N.D.	N.D.	16.7	102.1	0.512584 ± 9	–0.74
NBP-3	158.4	1178.9	0.70586 ± 9	0.70572	15.2	96.5	0.512606 ± 10	–0.3
Navajo volcanic field minette, northwestern New Mexico and northeast Arizona, Ship Rock–Twin Falls area (26–24 Ma)								
BR-1	130.2	994	0.705911 ± 11	0.70578	14.1	86.7	0.512612 ± 14	–0.19
Sr-6	127.5	1160.5	0.706606 ± 9	0.70649	18.1	110.7	0.512575 ± 13	–0.92
3BR	N.D.	N.D.	N.D.	N.D.	20.5	123.9	0.512544 ± 10	–1.53
Navajo volcanic field minette, southwest Colorado, Mesa Verde area (26–24 Ma)								
JC-14	136.8	746.6	0.705272 ± 12	0.70508	18.3	108.8	0.512653 ± 9	0.6
L-11-EL-WM-01[†]	158	1210	0.706131 ± 6	0.706	22.4	119	0.512648 ± 7	0.54
L-11-EL-WM-03[†]	159	1130	0.706152 ± 8	0.706	21.1	114	0.512639 ± 9	0.37
L-11-EL-WM-05[†]	142	1050	0.706189 ± 10	0.7061	18.7	99.8	0.512618 ± 8	–0.05
EM-1	120.1	1121.5	0.706554 ± 10	0.70644	19.9	116.8	0.512649 ± 10	0.51
Northern extent of Dulce dike swarm (kersantite) (25–20 Ma)								
DU-10	28.1	1650.9	0.705794 ± 7	0.70578	12.5	72.8	0.512244 ± 10	–7.45
DU-16	46.5	1247.1	0.705750 ± 7	0.70572	9.7	54.7	0.512411 ± 12	–4.2
Mafic dikes of the western San Juan Mountains (7–4 Ma), spessartite								
L-10-EL-FM-01C[†]	70.9	1180	0.706050 ± 12	0.7056	11	66.8	0.512648 ± 20	0.58
L-11-EL-CM-07[†]	39.8	1160	0.705227 ± 10	0.7052	12.4	68.5	0.512603 ± 11	–0.33
L-11-EL-CM-08[†]	40.5	1030	0.705127 ± 9	0.7051	12	70.5	0.512637 ± 14	0.36
Mafic dikes of the western San Juan Mountains (7–4 Ma), kersantite								
L-10-EL-FM-02[†]	56.7	1410	0.705485 ± 7	0.7054	12	71	0.512686 ± 3	1.32
L-10-EL-BB-01[†]	38.3	1160	0.705023 ± 6	0.705	10.8	65.4	0.512638 ± 4	0.38
L-10-EL-CM-04L[†]	39.2	1170	0.705284 ± 11	0.7052	11.8	72	0.512623 ± 7	0.1
LH-11	37.2	1007.9	0.705193 ± 9	0.70518	12.1	72.4	0.512588 ± 11	–0.88
L-11-EL-PV-01S[†]	65.4	1270	0.706710 ± 12	0.7067	12.7	66.5	0.512702 ± 16	1.58
PV-1	63.7	2003.6	0.708064 ± 13	0.70806	11.9	68	0.512700 ± 15	1.27
Specie Mesa basalt flow, western San Juan Mountains (614 ka)								
SPM-1	34.6	1288	0.704835 ± 9	0.70483	11.2	64.5	0.512662 ± 12	0.5
SPM-2	37.7	1190	0.704810 ± 7	0.70481	11.1	64.2	0.512629 ± 13	–0.2

N.D.—no data.
*Concentrations in parts per million.
[§]Ages used for time-corrected values: Navajo volcanic field (24 Ma), Dulce dikes (25 Ma), 7 Ma for mafic dikes in western San Juan Mountains except for dikes near Placerville (PV), for which a crystallization age of 4 Ma was used, and Specie Mesa basalt (1 Ma).
[†]Data were also reported in Lake and Farmer (2015).

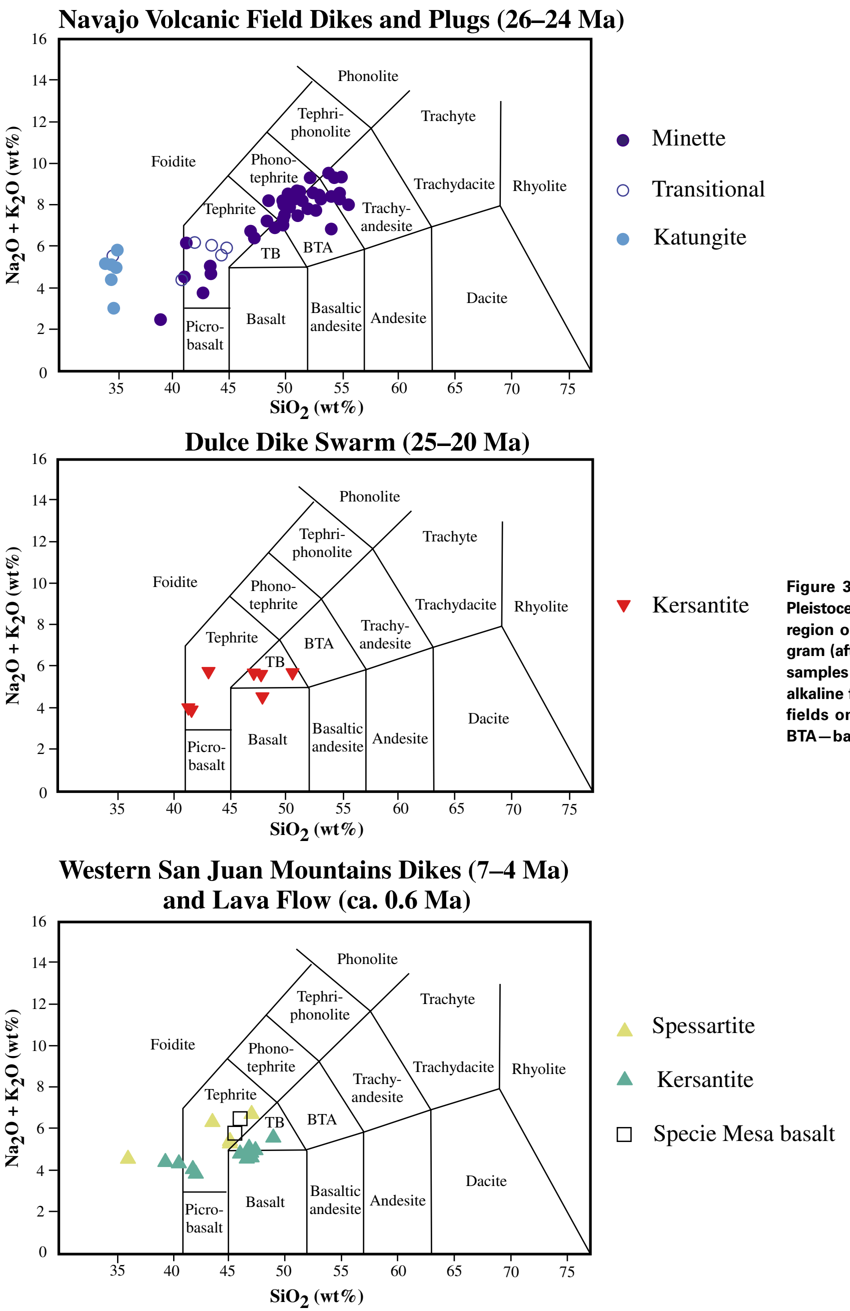

Figure 3. A comparison of Oligocene to Pleistocene mafic rocks in the Four Corners region on the total alkali versus silica diagram (after Le Bas et al., 1986). Most of the samples (Table 2), regardless of age, plot in alkaline field. Abbreviations used for some fields on the diagram: TB—trachybasalt; BTA—basaltic trachyandesite.

MAJOR-ELEMENT CHEMISTRY

Seventy-eight samples were analyzed for major- and trace-element geochemistry (Table 2); a summary of methods and analytical parameters are provided in the Appendix. The majority of the samples collected showed no visible signs of alteration in outcrop, and petrographic analyses confirmed an absence of alteration in most samples. The exceptions were several NVF and WSM samples in which olivine phenocrysts were partially altered to chlorite ± serpentine, and a few Dulce samples in which biotite and pyroxene were rimmed by secondary chlorite. Some of the outcrops sampled within the study area (Fig. 1) contain calcite in cavities, veins, and hydrothermal-breccia fillings. Field and petrographic evidence suggests that most of the calcite was related to magmatism and not to postmagmatic alteration. Irrespective of their origin, these calcite-rich zones were avoided during sampling. Petrographic analyses reveal that secondary calcite only occurs in the groundmass of some Dulce samples, which likely contributed to their high loss on ignition (LOI). The relatively high LOI values listed on Table 2 are similar to those (2–9 wt%) documented for "unaltered" alkaline mafic rocks worldwide (e.g., Roden and Smith, 1979; Leat et al., 1988; Wallace and Carmichael, 1989; Tingey et al., 1991; Gibson et al., 1992; Gibson et al., 1993; Nowell, 1993; Gibson et al., 1995; Righter and Rosas-Elguera, 2001; Kheirkhah et al., 2015). For phlogopite-bearing rocks, the high LOI is attributable, in part, to high modal proportions of phlogopite, which can contain up to 4–5 wt% H_2O^+ (table 18 in Deer et al., 1978; Alietti et al., 1995). The modal percentages of phlogopite (phenocrysts and groundmass) in our samples (Table 2), especially NVF rocks, vary from 10% to 40% and contributed to high loss of H_2O^+ during major-element analyses. Given the mineral assemblages in our samples, and lack of evidence for secondary alteration, we attribute the high LOI values to primary rock composition. The high LOI and low totals (~95%) for two of the WSM spessartite samples (L-10-EL-FM-01C and L-11-EL-CM-06; Table 2), however, are problematic. The major-oxide data for these two samples are listed on Table 1 and plotted on the various diagrams, but these data are questionable.

The wide range of crystallization ages (2–7 m.y.) for mafic rocks in any given field (Tables 1 and 2) makes it difficult to assess magmatic relationships of the rocks and complicates the use of chemical models for quantitative assessment of differentiation processes such as crystal fractionation. Models to assess different degrees of source melting are also inhibited by the lack of trace-element compositions for mantle peridotites found in the region. Nevertheless, general geochemical patterns are defined by our data, and these allow a qualitative assessment of source heterogeneity and contamination processes.

Most of the samples we analyzed (Table 2) plot in the alkaline field on the total alkali silica (TAS) diagram (Fig. 3) (Le Maitre et al., 1989). There is a wide range of SiO_2 (34–58 wt%) and $Na_2O + K_2O$ (2–10 wt%) on the plots with considerable overlap of data amongst the three rock groups (Table 2). Samples from the Navajo volcanic field show the greatest spread on the TAS plot, but there is also notable variation for the WSM and Dulce samples.

For all samples analyzed (Table 2), there is a wide range of Mg# values (80–40, defined as 100*[Mg^{2+}/(Mg^{2+} + Fe^{2+}]) relative to SiO_2 concentrations of 34–58 wt% (Fig. 4). The NVF samples are distinguished by a continuum of SiO_2 from 34 to 55 wt% with Mg# from 60 to 80. Most of the WSM and Dulce samples have 40–55 wt% SiO_2, but the Mg# for a majority of WSM rocks is 55–65, whereas those for the Dulce samples plot around 50. The K_2O versus SiO_2 plot (Fig. 4, boundaries from Peccerillo and Taylor, 1976) highlights the distinctions between the different rock groups, despite some overlap. Navajo volcanic field katungites with 34–35 wt% SiO_2 and 1.5–3.5 wt% K_2O plot in a distinct cluster in the low-silica range of the shoshonite field. Most of the NVF minettes are ultrapotassic and plot in the shoshonitic field but have a wider range in K_2O concentrations compared to the katungites. Minette samples with the lowest SiO_2 overlap the field of NVF transitional rocks in the low K_2O part of the shoshonitic field, as do the majority of the WSM samples. In contrast, the Dulce samples plot from the shoshonitic field into the high- to medium-K fields, reflecting their overall lower K_2O concentrations (Table 2).

Navajo volcanic field katungites are the least evolved of all rock types with 33–37 wt% SiO_2, high Mg#, and highest overall wt% MgO, FeO*, and CaO (Fig. 4). The katungites have relatively uniform K_2O/Na_2O from 1.03 to 1.95, and are distinguished by high proportions (wt%) of normative olivine (18.4–27.3), nepheline (5.7–10.5), and leucite (8.2–13.7). Navajo volcanic field minettes show the greatest variation in major-element chemistry but overall are silica undersaturated and potassic to ultrapotassic with K_2O/Na_2O of 0.70–4.84. These chemical trends are reflected by variable but generally high normative orthoclase (12.2–43.3 wt%), and normative nepheline (0.1–12.2 wt%), in most samples. Navajo volcanic field transitional rocks plot between the katungites and minettes on the Harker diagrams (Fig. 4) and are distinguished by normative olivine (3.1–11.5 wt%) + nepheline (2.8–7.4 wt%) ± leucite (2.7–22.8 wt%), and Or > (An + Ab).

The major-element oxides of NVF minette + transitional samples define distinct linear trends. With increasing SiO_2 concentrations, there are positive correlations for Al_2O_3, K_2O, and Na_2O and negative correlations for MgO, FeO*, CaO, and TiO_2. Nowell (1993) argued for 11% to 21% closed-system crystal fractionation of diopside + phlogopite + apatite + magnetite from primary melts to produce the range of chemical compositions in NVF minettes. Alibert et al. (1986) also interpreted the variations in MgO, Cr, Ni, and REE as the result of fractionation of olivine + pyroxene from primary melts, and Roden et al. (1990) proposed that chemical variations in minettes at Buell Park were caused by fractional crystallization of primitive melts derived from sources that were isotopically heterogeneous. These models define samples with high MgO, Ni, and Cr as representatives of primitive or primary mantle melts. A challenge to this assumption comes from several experimental studies (Wyllie and Sekine, 1982; Sekine and Wyllie, 1983; Lloyd et al., 1985). These experiments produced a wide range of alkaline melt compositions by partial melting of heterogeneous subcontinental mantle composed of phlogopite + clinopyroxene + orthopyroxene without involving crystal fractionation from a "primary" melt. The linear variations in major- and trace-element compositions for NVF minettes hint that fractional crystallization was a factor, but it probably was not the primary cause of all of the chemical variation observed. In contrast to the NVF minettes and transitional rocks, the Dulce and WSM data (Table 2) do not exhibit well-defined trends (Fig. 4).

Western San Juan Mountains spessartites are distinguished by generally higher Al_2O_3 and K_2O and a wider range of K_2O/Na_2O (0.36–6.58) relative to WSM kersantites (0.81–2.82). Most of the WSM dike rocks and the Specie Mesa basalt (Table 2) are distinguished by normative (Ab + An) >> Or, olivine (0.6–10.6 wt%), nepheline (0.1–12.1 wt%) ± leucite (0.9 wt%). Major-element values for the Specie Mesa basalt (Tables 1 and 2) mostly plot in the clusters defined by the Dulce samples (Fig. 4).

The Dulce rocks generally have lower Mg#, CaO, K_2O, and K_2O/Na_2O (0.12–1.36) relative to NVF and WSM rocks (Fig. 4). Most of the samples have normative (Ab + An) >> Or + olivine + nepheline, but four samples (DU3, DU5, DU6, and DU10; Table 2) are quartz normative (0.7–1.6 wt%). The normative quartz could be attributed to crustal contamination in these rocks.

TRACE-ELEMENT CHEMISTRY

Plots on Figure 5 further reveal the distinct groupings of chemical data for different mafic rock suites in the region (Fig. 2; Table 2). On the plot of La/Ta versus K_2O (Fig. 5A), the Dulce samples have the lowest K_2O with La/Ta ratios of 10–90, and the data cluster around average regional lower crust. Most of the NVF katungites plot in the upper extent of the oceanic island basalt (OIB) field with La/Ta ratios of 0–40 and 1–4 K_2O, together with a few NVF minette samples and most of the WSM rocks. The majority of the NVF minette and transitional samples have K_2O from 3 to 8 wt% and a greater range in La/Ta (10–150). The variations in K_2O could in part be attributable to fractional crystallization, but the fields defined are consistent with heterogeneous mantle sources. The data for Dulce dike rocks are compatible with mixing of mantle melts and lower crust.

A plot of La/Ta against K/Ta*1000 (Fig. 5B) shows a continuum from NVF katungites (OIB) on the lower end of the K/Ta spectrum to NVF minettes on the upper end. The overall trends are similar to the results defined by Leat et al. (1988) for middle to late Cenozoic mafic rocks in northwestern Colorado (Fig. 1); the sources for these rocks were interpreted as asthenospheric (OIB) (Group 1) to subcontinental mantle (Group 2).

The plot of Ta/Yb against Th/Yb (Fig. 5C) after Pearce (1983; Pearce and Peate, 1995) also displays distinct fields with well-defined ranges in Th/Yb for all three rock groups. Navajo volcanic field katungites plot in the upper part of the mantle array in the OIB field, whereas the majority of the NVF minettes and transitional rocks plot between the katungites and potassic "arc" rocks (shoshonitic field). Although the Th/Yb ratios for the WSM and Dulce samples are lower than for NVF samples, there is a similar shift in the Ta/Yb ratios from enriched mantle into the shoshonitic and calc-alkaline fields. The overall trends defined on this plot might be explained by variable mixing of melts from enriched asthenospheric mantle and metasomatized lithospheric mantle or heterogeneity in mantle sources.

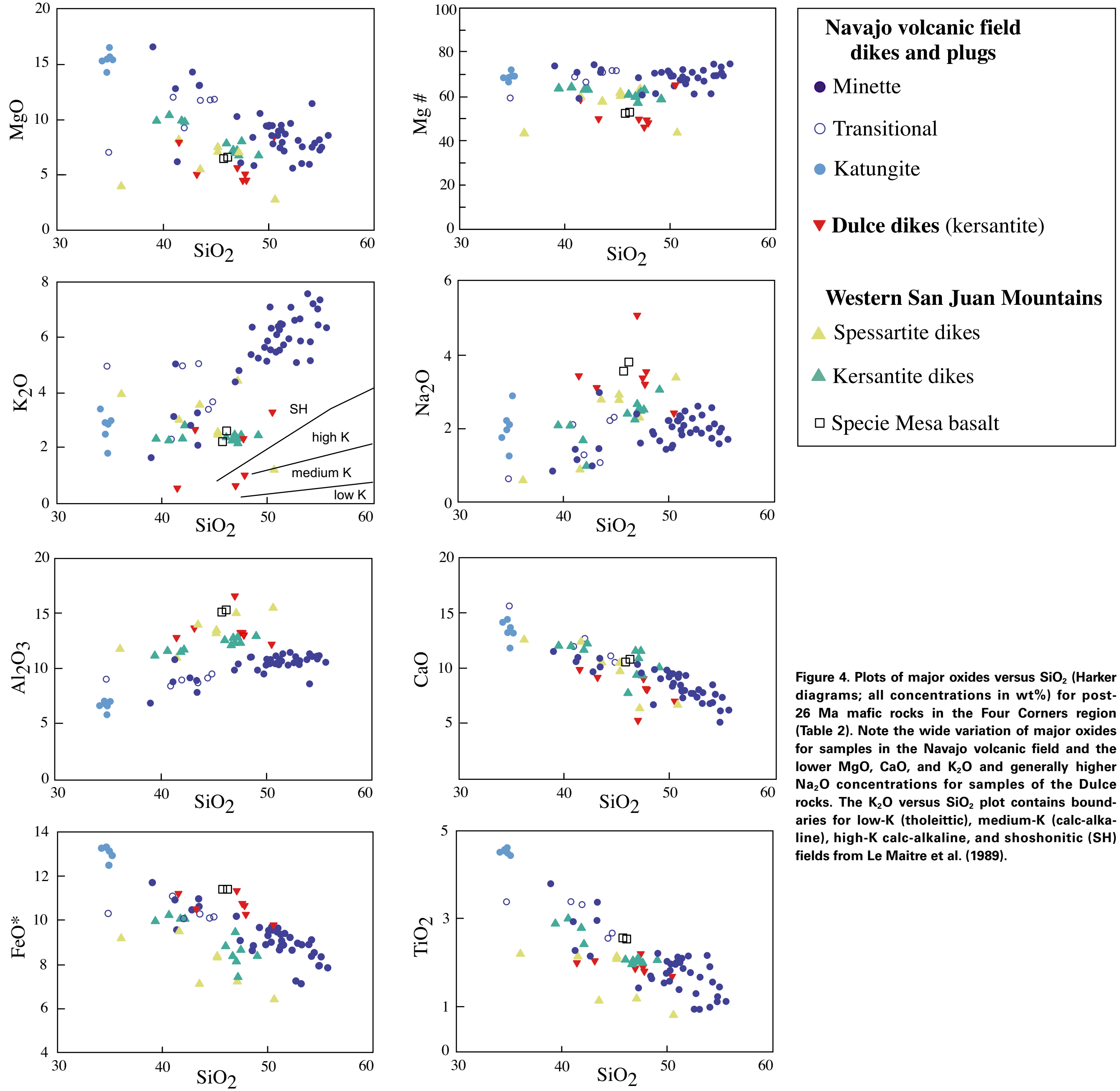

Figure 4. Plots of major oxides versus SiO_2 (Harker diagrams; all concentrations in wt%) for post-26 Ma mafic rocks in the Four Corners region (Table 2). Note the wide variation of major oxides for samples in the Navajo volcanic field and the lower MgO, CaO, and K_2O and generally higher Na_2O concentrations for samples of the Dulce rocks. The K_2O versus SiO_2 plot contains boundaries for low-K (tholeiitic), medium-K (calc-alkaline), high-K calc-alkaline, and shoshonitic (SH) fields from Le Maitre et al. (1989).

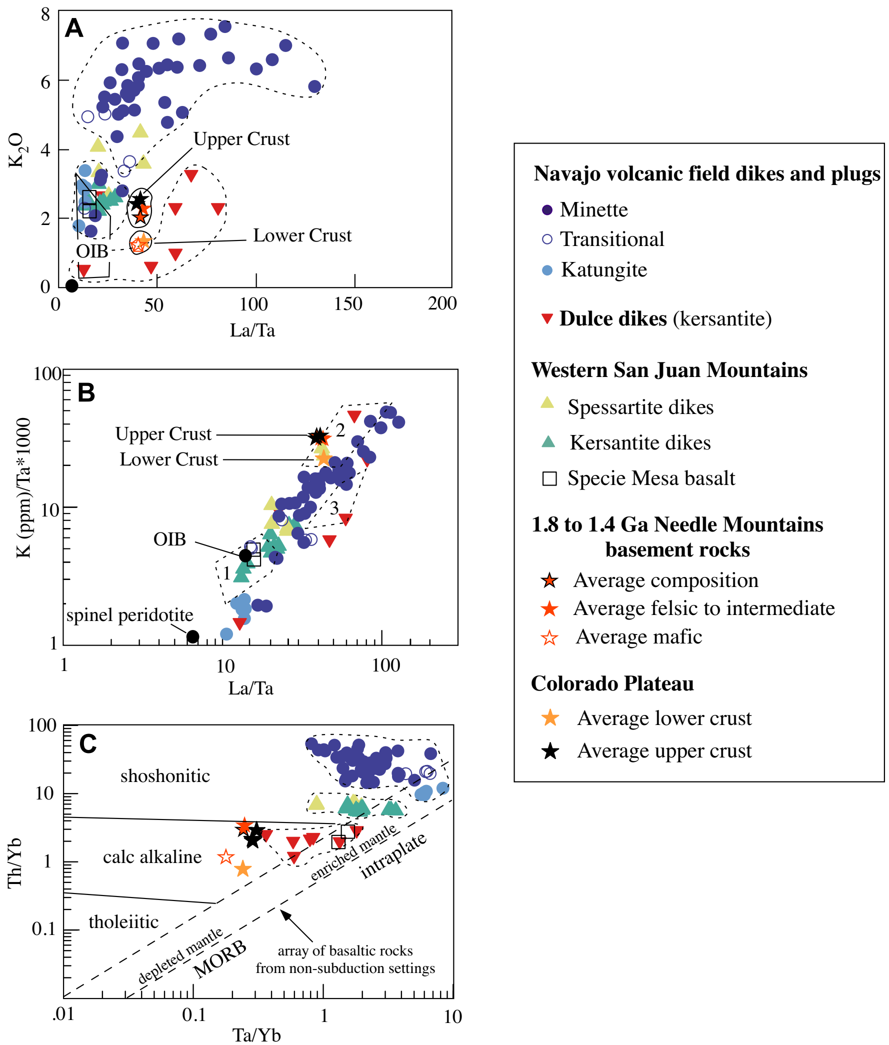

Figure 5. Plots of (A) La/Ta versus K_2O wt%; (B) La/Ta versus K (ppm)/Ta*1000; and (C) Ta/Yb versus Th/Yb (after Pearce, 1983) that illustrate the groupings of different mafic rocks investigated. The data on the plots define three distinct fields that lend evidence for heterogeneity in mantle sources. On the plot of La/Ta versus K (ppm)/Ta*1000, the mantle fields that were defined with geochemical data for Oligocene to Miocene rocks in the northern extent of the Rio Grande rift (Leat et al., 1988) are shown for comparison: ocean island basalt (OIB) (Group 1, 12 Ma to present), subcontinental lithospheric mantle (Group 2, 12–7 Ma), and metasomatized OIB (Group 3, 24–7 Ma). The plot of Ta/Yb versus Th/Yb illustrates the distinct trend from the alkalic rocks of the Navajo volcanic field (NVF) to the subalkalic rocks of the Dulce field and the gradation of data for each group from the enriched mantle array (OIB) to the shoshonitic field or calc-alkaline fields. The field for OIB in (A) is from Thompson et al. (1993). The average compositions for primitive mantle, OIB, and normal-type mid-ocean ridge basalt (N-MORB) are from Sun and McDonough (1989), and the average composition for spinel peridotite (proxy of subcontinental lithospheric mantle (SCLM) is from McDonough (1990). Compositional data for the upper and lower crust of the Colorado Plateau are from geochemistry of xenoliths reported by Condie and Selverstone (1999).

Plots of La/Lu relative to concentrations of compatible (Ni and Cr) and more incompatible trace elements (Ba, Nb, Rb, and Zr) (Fig. 6) for samples show a wide variation in concentrations over a range of La/Lu from 50 to 1000. Ba and Zr show a general positive correlation with increasing La/Lu, for all samples, but there are no definitive trends for the other elements. Katungite samples have the least amount of element variation and higher overall Nb, Ni, Cr, and Zr concentrations. There is a general progressive decrease in La/Lu and element concentrations from NVF > WSM > Dulce samples.

The chondrite-normalized, rare-earth element (Sun and McDonough, 1989) (Fig. 7) patterns for all samples display an enrichment in light rare-earth elements (LREEs) relative to heavy rare-earth elements (HREEs) (La_N/Yb_N = 10–100) and relatively flat HREE patterns (Dy_N/Yb_N = 1.2–1.5). A subset of NVF minette-transitional rocks has the highest normalized LREE, whereas the lowest are exhibited by several samples of WSM samples. These patterns are similar to those of potassic magmas formed in subduction margins.

Mid-ocean ridge basalt (MORB)–normalized multi-element plots (after Pearce, 1983) (Fig. 8) show variable but overall high enrichment in incompatible large-ion lithophile elements (LILEs). The patterns for NVF katungite samples are broadly similar to those for oceanic island basalts but with higher LILE and LREE. Navajo volcanic field minette-transitional samples are slightly more enriched in LILE compared to WSM or Dulce samples. Excluding the katungite samples, the MORB-normalized patterns for all samples are distinguished by moderate to pronounced negative Ta-Nb troughs and subtle Zr-Hf negative anomalies that are similar to patterns of rocks generated in continental arcs. Roden et al. (1990) argued that Ta-Nb depletion in "felsic" minettes (sanidine rich) in the NVF could reflect fractionation of Ta-Nb–rich mineral phases from more primitive magmas, but this is not supported by the fact that some NVF minettes (samples at Johnson Canyon, Red Wash, and Boundary Butte) with high proportions of sanidine and phlogopite have higher Nb concentrations relative to olivine-bearing minettes (Table 2). Tingey et al. (1991) proposed that the Ta-Nb troughs could simply be the results of enrichment of LILE and LREE relative to Ta and Nb (and Zr-Hf) in a metasomatized source that interacted with enriched fluids or magmas. For the NVF transitional and minette samples, the normalized Th values define distinct peaks on the MORB-normalized plots relative to Ta and Ba, whereas the WSM and Dulce samples lack this pronounced Th enrichment. The lower normalized Th could be explained by fractionation of phlogopite, hornblende, or pyroxene from the melts or the presence of a Th-rich mineral in the melt source.

Sr-Nd ISOTOPE SIGNATURES

Age-corrected Sr and Nd isotopic ratios for samples from the different rock groups (Table 3) have higher $^{87}Sr/^{86}Sr_{(i)}$ ratios and lower $\varepsilon_{Nd\,(t)}$ with respect to depleted asthenospheric mantle (MORB) (Fig. 9). Relative to bulk silicate earth (BSE), the majority of the isotopic data (Table 3) are moderately radiogenic in $^{87}Sr/^{86}Sr_{(i)}$ (0.7050–0.7060) and slightly enriched or depleted in $^{143}Nd/^{144}Nd$, giv-

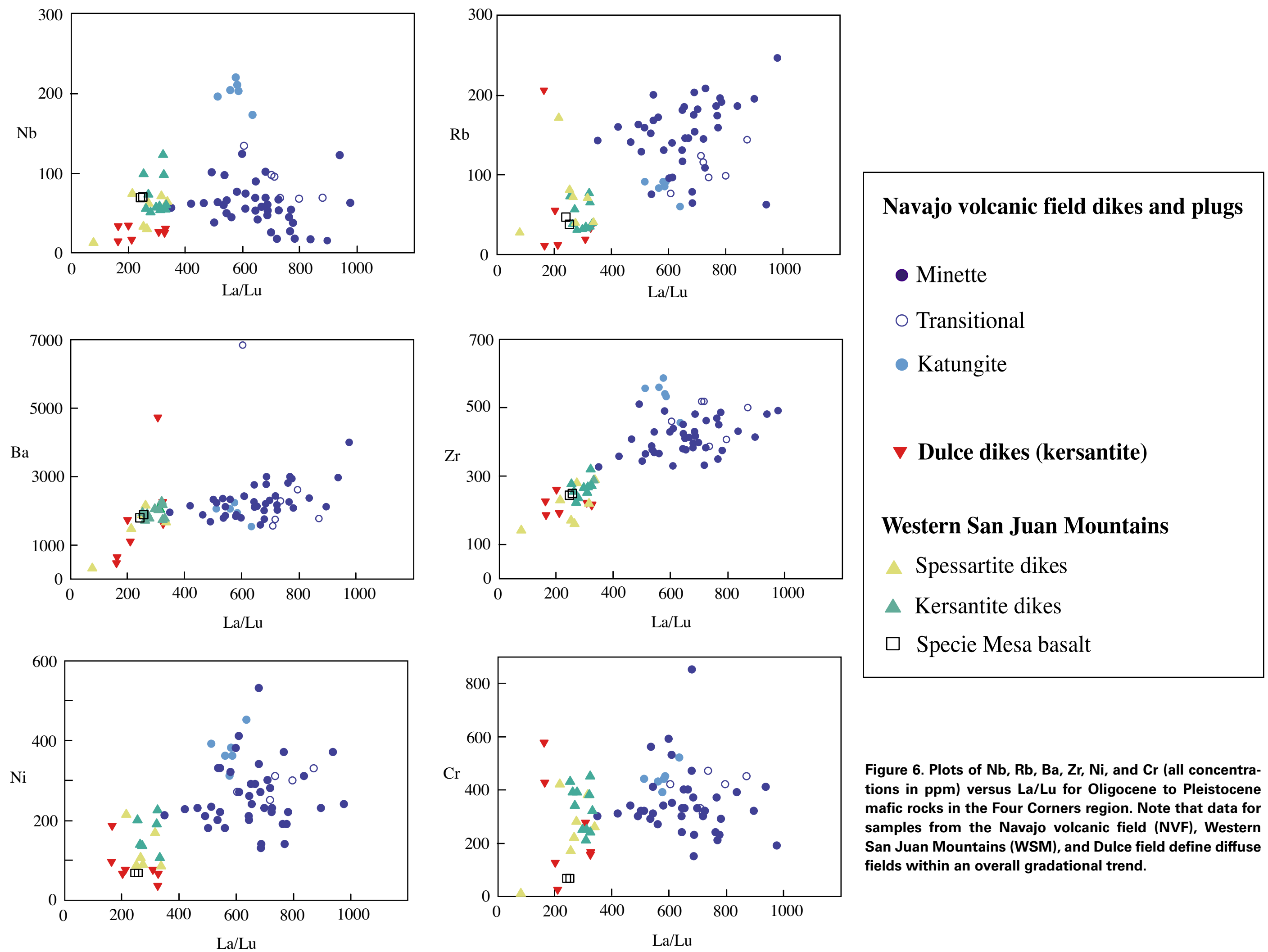

Figure 6. Plots of Nb, Rb, Ba, Zr, Ni, and Cr (all concentrations in ppm) versus La/Lu for Oligocene to Pleistocene mafic rocks in the Four Corners region. Note that data for samples from the Navajo volcanic field (NVF), Western San Juan Mountains (WSM), and Dulce field define diffuse fields within an overall gradational trend.

ing $\varepsilon_{Nd(t)}$ values of +2 to −2. These trends are analogous to those documented in some Oligocene to Pliocene alkaline mafic rocks in northwestern Colorado (Fig. 1), defined by increasing Sr isotope compositions (0.703–0.707) and near-constant $^{143}Nd/^{144}Nd$ (0.5122–0.5124) (Leat et al., 1988). The variable $\varepsilon_{Nd(t)}$ with increasing $^{87}Sr/^{86}Sr_{(i)}$ in the majority of NVF and WSM samples (Fig. 9) indicates that lithospheric mantle source was heterogeneous or there was contamination of the melts by upper continental crust as argued by Leat et al. (1988) for the mafic rocks in northwestern Colorado (Fig. 1).

Bulk-rock Nd and Sr isotope data for NVF samples (Table 3) are similar to data reported in previous publications (Alibert et al., 1986; Roden et al., 1990; Nowell, 1993; Carlson and Nowell, 2001). Minette and transitional samples mostly plot within the field delineated for the Colorado Plateau subcontinental lithospheric mantle (SCLM on Fig. 9), which straddles BSE. Several of the NVF katungites have lower $^{87}Sr/^{86}Sr_{(i)}$ ratios at ~0.7039 and plot between the average field for OIB and PREMA (prevalent mantle of Zindler and Hart [1986]) and BSE (Rollinson, 1993).

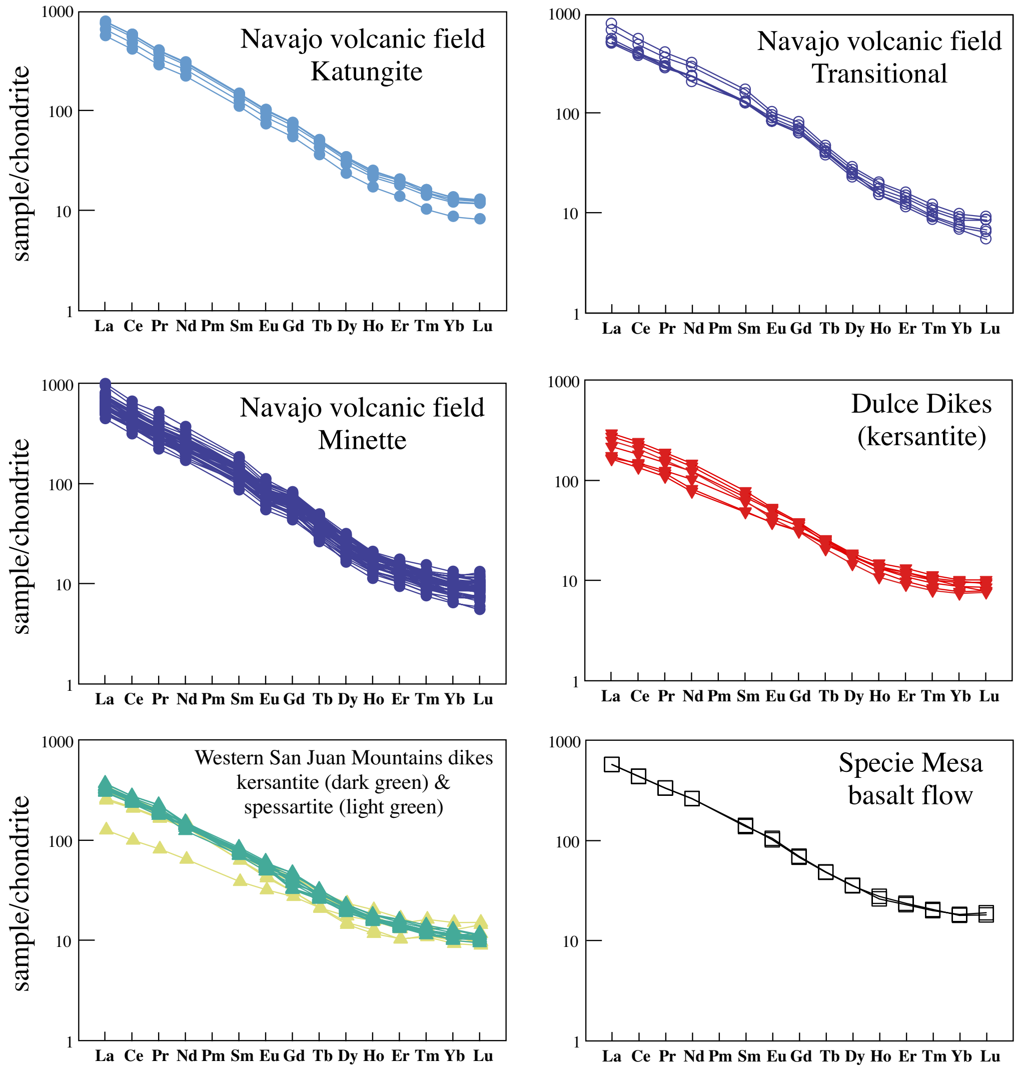

Figure 7. Comparison of chondrite-normalized, rare-earth element abundances for Oligocene to Pleistocene mafic rocks analyzed in this study. Normalizing element concentrations are from Sun and McDonough (1989).

Nd and Sr isotopic data for the majority of the WSM dike rocks, and Specie Mesa basalt, cluster around BSE within the field defined by NVF data. Pb isotopic data reported for some WSM rocks (Lake and Farmer, 2015) also overlap the range of Pb isotopic data for NVF minettes (Carlson and Nowell, 2001) and are significantly more radiogenic than the depleted mantle. Several WSM samples have higher $^{87}Sr/^{86}Sr_{(i)}$ ratios (0.706710 and 0.708064), which could reflect minor contamination with ^{87}Sr-rich upper continental crust (Fig. 9; Table 3). The Dulce samples (Table 3) are distinguished by near-constant $^{87}Sr/^{86}Sr_{(i)}$ values (~0.706) and $\varepsilon_{Nd(t)}$ values of –4.2 to –7.5. These $\varepsilon_{Nd(t)}$ values are more negative than those reported for samples of Dulce dikes in northern New Mexico (–2.6 to –3.3 in Gibson et al., 1993).

Roden et al. (1990) argued against crustal contamination as the cause of variation in $^{87}Sr/^{86}Sr_{(i)}$ in NVF minettes at Buell Park. They cited the positive correlation of Ce/Yb ratios with increasing $\varepsilon_{Sr(t)}$ (noted by Alibert et al., 1986)

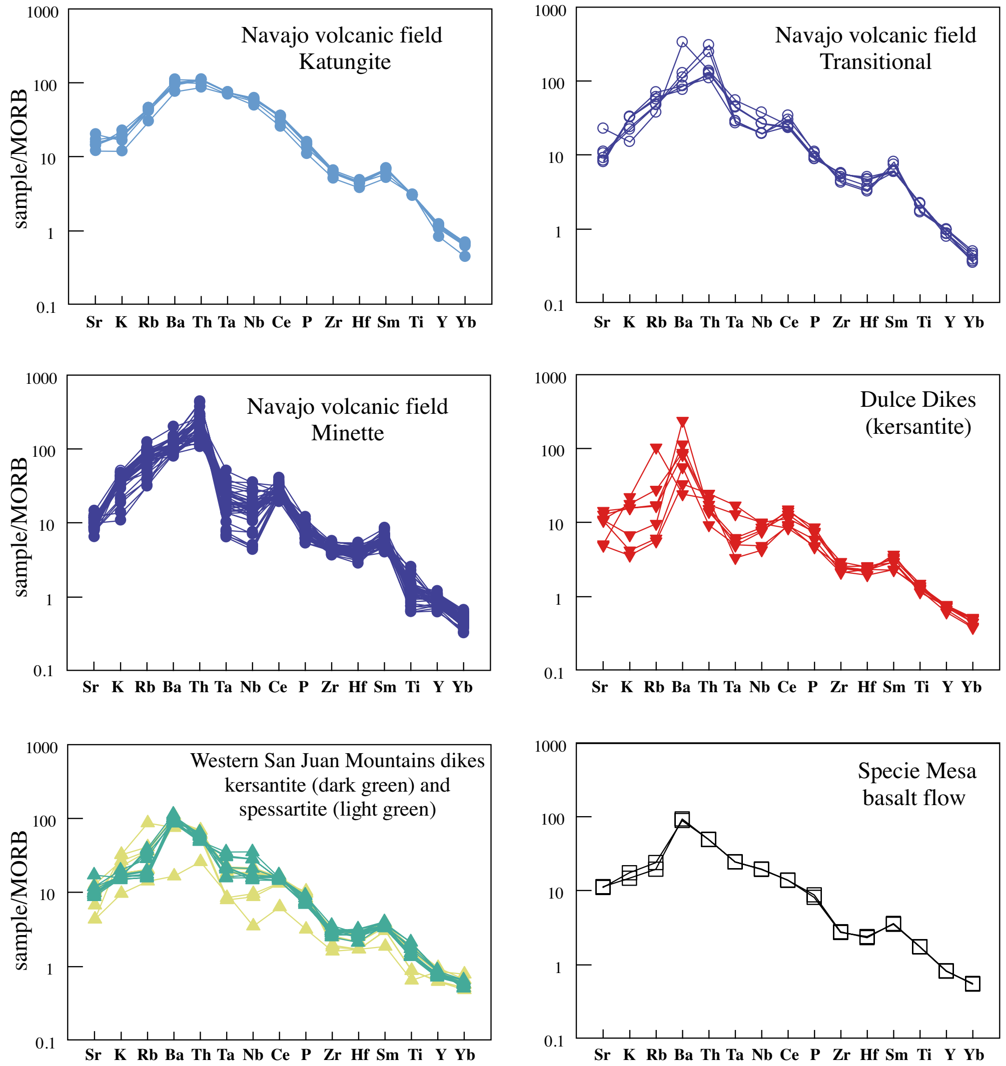

Figure 8. Comparison of mid-ocean ridge basalt (MORB)-normalized element abundances for the post-26 Ma mafic rocks from the Four Corners region. Normalizing element concentrations are from Pearce (1983).

as supporting evidence, since contamination with upper crustal rocks is expected to produce low Ce/Yb ratios. Roden et al. (1990) proposed instead that the variations in $^{87}Sr/^{86}Sr_{(i)}$ ratios were likely caused by minor source heterogeneity, a hypothesis that was further supported by isotopic studies of Alibert et al. (1986), Nowell (1993), and Carlson and Nowell (2001).

The variations in Nd and Sr isotopic compositions of post-26 Ma rocks in the Four Corners region (Fig. 2) could reflect heterogeneity in melt sources or different degrees of crustal contamination. We contend that contamination of melts by upper continental crust was not significant. The high Sr concentrations for most of the mafic melts (900–2500, Table 2) would tend to buffer the effects of contamination by crustal rocks with low Sr concentrations. Our model-mixing line (Fig. 9) between the regional SCLM and average upper continental crust indicates that the Sr isotopic ratios of several WSM samples could be produced by contamination of mantle melts with less than ~0.6%

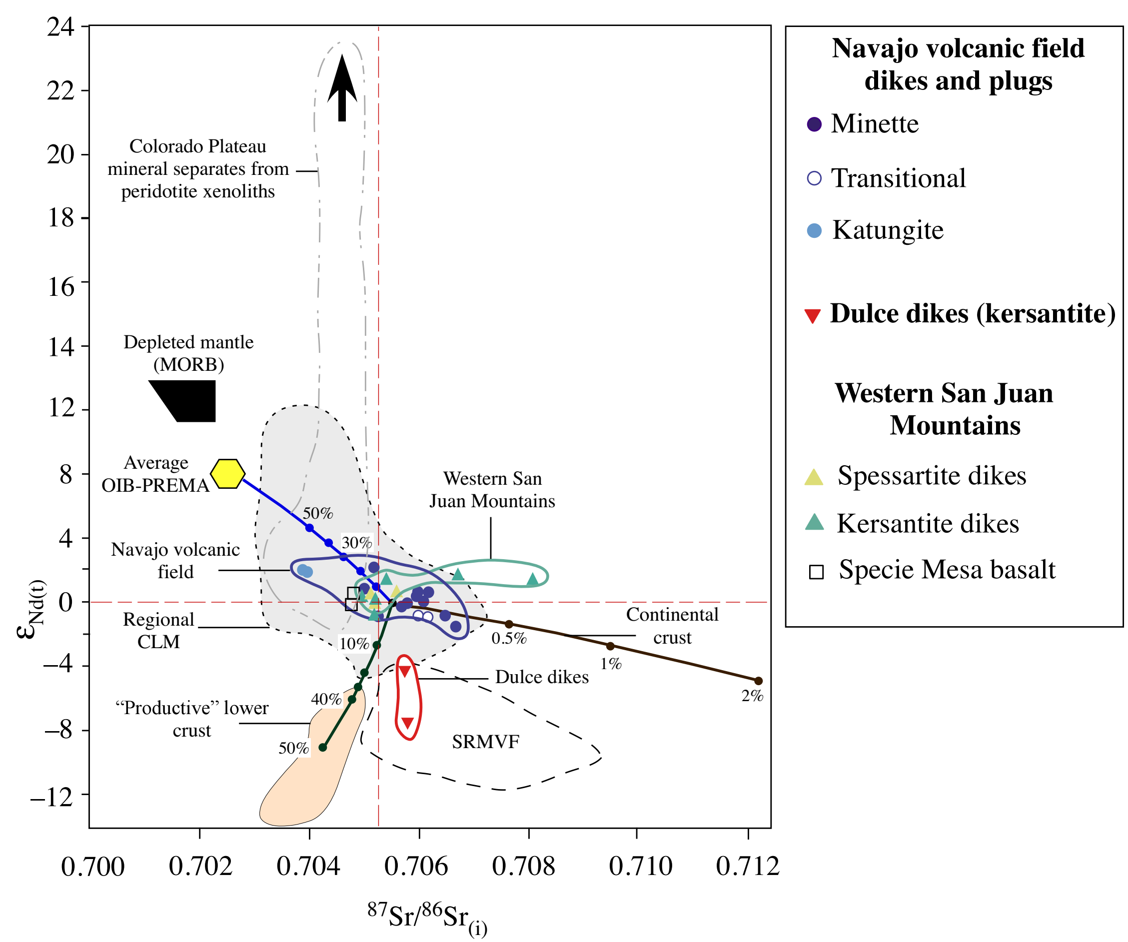

Figure 9. Epsilon Nd(t) versus $^{87}Sr/^{86}Sr_{(i)}$ plot for Oligocene to Pleistocene mafic rocks in the Four Corners region (Table 3). Bulk silicate earth is defined at ε_{Nd} = 0 and $^{87}Sr/^{86}Sr$ = 0.7052. Sources for different fields: (1) subcontinental lithospheric mantle (SCLM shown in gray) beneath the Colorado Plateau and (Alibert et al., 1986; Roden et al., 1990; Nowell, 1993; Carlson and Nowell, 2001); (2) northern Colorado (Bailley, 2010); (3) "Productive" Lower Crust (Lake, 2013); (4) Southern Rocky Mountains volcanic field (SRMVF) (Riciputi et al., 1995; Lake and Farmer, 2015); and (5) mid-ocean ridge basalt (MORB) and prevalent mantle (PREMA) (Zindler and Hart, 1986; Rollinson, 1993). The upper extent of the SCLM field beneath the Colorado Plateau is defined by isotopic analyses on clinopyroxene and amphibole from peridotite xenoliths in the Grand Canyon area (Alibert, 1994; Riter, 1999), and several samples of clinopyroxene and amphibole from garnet peridotite collected at the Thumb (Alibert, 1994) and Green Knobs (Roden et al., 1990) in the Navajo volcanic field (NVF). The arrow at the top of the field shows that the ε_{Nd} for the field extends to +145 with $^{87}Sr/^{86}Sr$ from 0.7038 to 0.7047. Riter (1999) argued that the time-integrated light rare-earth element (LREE) depletion in diopside separates from some peridotite xenoliths indicated that zones in the lithospheric mantle beneath the Colorado Plateau were depleted by: (1) melting events in the Proterozoic; (2) a high degree of mantle melting in the Cenozoic; or (3) a combination of these processes. The first option was favored to explain the high ε_{Nd} values, but Riter (1999) noted that the peridotites were also subjected to later period of metasomatism and Sr enrichment during slab dehydration. The heavy blue line on the plot is a mixing curve that we generated by applying simple binary-liquid mixing. The model assumes that the primary melts had the same chemical composition as SCLM and ocean island basalt (OIB). The heavy black lines are Energy-Constrained Assimilation Fractional Crystallization (EC-AFC) models (after Spera and Bohrson, 2001). Model calculations assumed 100% SCLM melt with progressive mixing or assimilation of OIB-PREMA, "productive" lower crust, and average continental crust. The EC-AFC model curves are marked with percentage increments.

upper crust. The overall variations in the isotopic signatures, however, do not lend support to significant contamination with upper crust. Further evidence against such contamination is provided by $^{87}Sr/^{86}Sr_{(m)}$ ratios of clinopyroxene (cpx) crystals in selected samples of NVF minette and transitional rocks (Fig. 10; Table 4). Similar core to rim $^{87}Sr/^{86}Sr_{(m)}$ ratios in the crystals show that there were no notable changes in the isotopic compositions of the melts during crystallization, as would be expected if crustal assimilation happened.

The Sr and Nd isotope data of Dulce samples could indicate variable contamination of mantle melts by mafic lower crust with low time-integrated Sm/Nd (e.g., as documented by Dungam et al., 1986; Johnson et al., 1990; Johnson and Thompson, 1991). The model-mixing line between SCLM and lower "productive" crust shows it is plausible that the Dulce samples were contaminated with 10% to 45% lower crust and up to 0.5% upper crust (Fig. 9). A similar process of lower crustal contamination is argued for basalts on the southern edge of the Colorado Plateau (Alibert et al., 1986), and Pliocene basalts erupted on the Taos Plateau in New Mexico (Dungan et al., 1986). Alternatively, the Dulce magmas could have originated from melting of a mantle source with a composition similar to lower mafic crust.

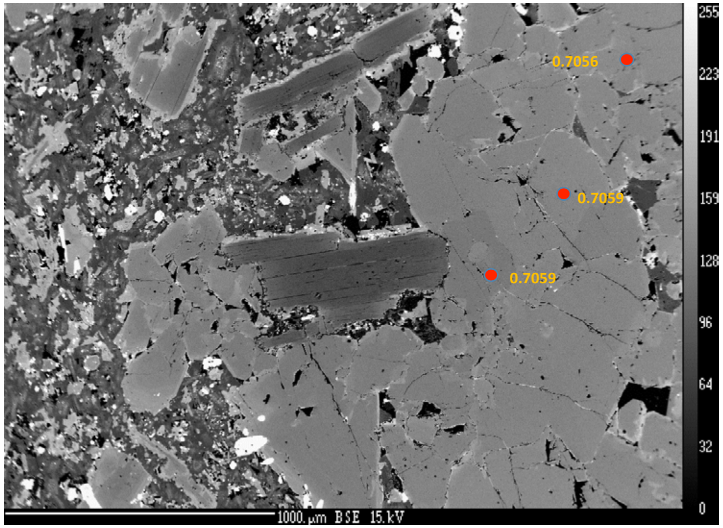

MV-WC1-04 SH13

Figure 10. Core-to-rim Sr isotopic ratios in a crystal of clinopyroxene (cpx) from a minette dike exposed at Weber Mountain (Fig. 2; Table 4). The similarity of the ratios from core to rim indicates that the magma did not undergo crustal contamination during emplacement and crystallization. Similar trends were noted in several cpx crystals from minette and transitional rocks sampled at different locations in the Navajo volcanic field (NVF) (Table 4).

Plots of Nd and Sr isotope data against SiO_2, Th/Yb, and La/Nb (Fig. 11) are used to further assess the influence of different mechanisms (source heterogeneity, crustal contamination, and fractional crystallization) on magma compositions. The varied and negative $\varepsilon_{Nd(t)}$ and similar $^{87}Sr/^{86}Sr_{(i)}$ with increasing SiO_2 for the Dulce samples (Fig. 11; Table 3) are compatible with contamination of mantle magmas by lower crust with low time-integrated Sm/Nd or melting of mantle rocks with a similar composition. The slight increase in $^{87}Sr/^{86}Sr_{(i)}$ and minor decrease in $\varepsilon_{Nd\ (t)}$ with increasing SiO_2 for NVF samples are consistent with heterogeneity in mantle sources or minor contamination with upper crust. Some WSM samples plot on a trend of increasing $^{87}Sr/^{86}Sr_{(i)}$ with near-constant SiO_2, while other samples plot on a trend of similar $^{87}Sr/^{86}Sr_{(i)}$ with increasing SiO_2. Neither of these trends support contamination of melts with upper continental crust but could reflect compositional variations in the mantle source. Plots of $^{87}Sr/^{86}Sr_{(i)}$ against Th/Yb and La/Nb (Fig. 11) also do not reveal trends indicative of crustal contamination. Since the Th/Yb and La/Nb ratios in mantle-derived rocks are sensitive to contamination of typical continental crustal with higher LREEs/high field strength elements (HFSEs) (Taylor and McLennan, 1985), a distinct relationship of higher $^{87}Sr/^{86}Sr_{(i)}$ with increasing element ratios are expected. A few NVF samples with high $^{87}Sr/^{86}Sr_{(i)}$ show slight increases in La/Nb that might reflect contamination, but the majority of the data do not. Navajo volcanic field katungites and WSM dike rocks with variable $^{87}Sr/^{86}Sr_{(i)}$ and similar La/Nb and Th/Yb ratios could, however, be explained by compositional diversity in the mantle source.

TABLE 4. CORE TO RIM STRONTIUM ISOTOPE DATA FOR DIOPSIDE IN MINETTE AND TRANSITIONAL SAMPLES, NAVAJO VOLCANIC FIELD

Sample number	$^{87}Sr/^{86}Sr_{(m)}$	2σ error in 4th decimal point
Newcomb		
NC-1 SP8.1	0.7054	2
NC-1 SP8.2	0.7053	1
NC-1 SP8.3	0.7056	2
Red Wash		
RW-3 SP4.1	0.7058	1
RW-3 SP4.2	0.7057	1
Red Wash		
RW-3 SP6.1	0.7057	1
RW-3 SP6.2	0.7055	1
Weber Mountain		
WM1-04 SP13.1	0.7056	1
WM1-04 SP13.2	0.7059	1
WM1-04 SP13.3	0.7059	1

Except for the Dulce dike samples, overall trends in our Nd and Sr isotopic data do not provide definitive support for contamination by continental crust, although we cannot exclude the possibility of minor assimilation during emplacement. We suggest that the trends are explained mostly by heterogeneity in the melt sources.

DISCUSSION

Oligocene to Pleistocene alkaline mantle melts were emplaced along the eastern margin of the Colorado Plateau in three separate fields (NVF, Dulce, and WSM) (Figs. 1 and 2) during intraplate regional extension, following subduction of the Farallon plate in the western United States (Fig. 12). Major- and trace-element data (Table 2) for rocks from each field reveal (Figs. 4–6) distinctions in magma compositions. This is contrasted by the similarity of Nd and Sr isotopic signatures, regardless of age. The chemical data also show that melts were enriched in LILE and LREE compared to depleted mid-oceanic ridge basalt (Fig. 5), indicating a long-term contribution of SCLM to mantle magmatism after 26 Ma.

Navajo volcanic field katungites have distinct chemical compositions relative to other mafic rocks in the Four Corners (e.g., lack of Ta-Nb depletion on Fig. 8). The hypothesis that the katungites formed by <2% melting of carbonated lithospheric peridotite with OIB affinities (Alibert et al., 1986; Roden et al., 1990; Nowell, 1993; Carlson and Nowell, 2001) is supported by the low SiO_2, high CaO, high Zr/Hf, and low La/Ta (e.g., Rudnick et al., 1993). In addition, the chemical data for these rocks consistently cluster within or near the

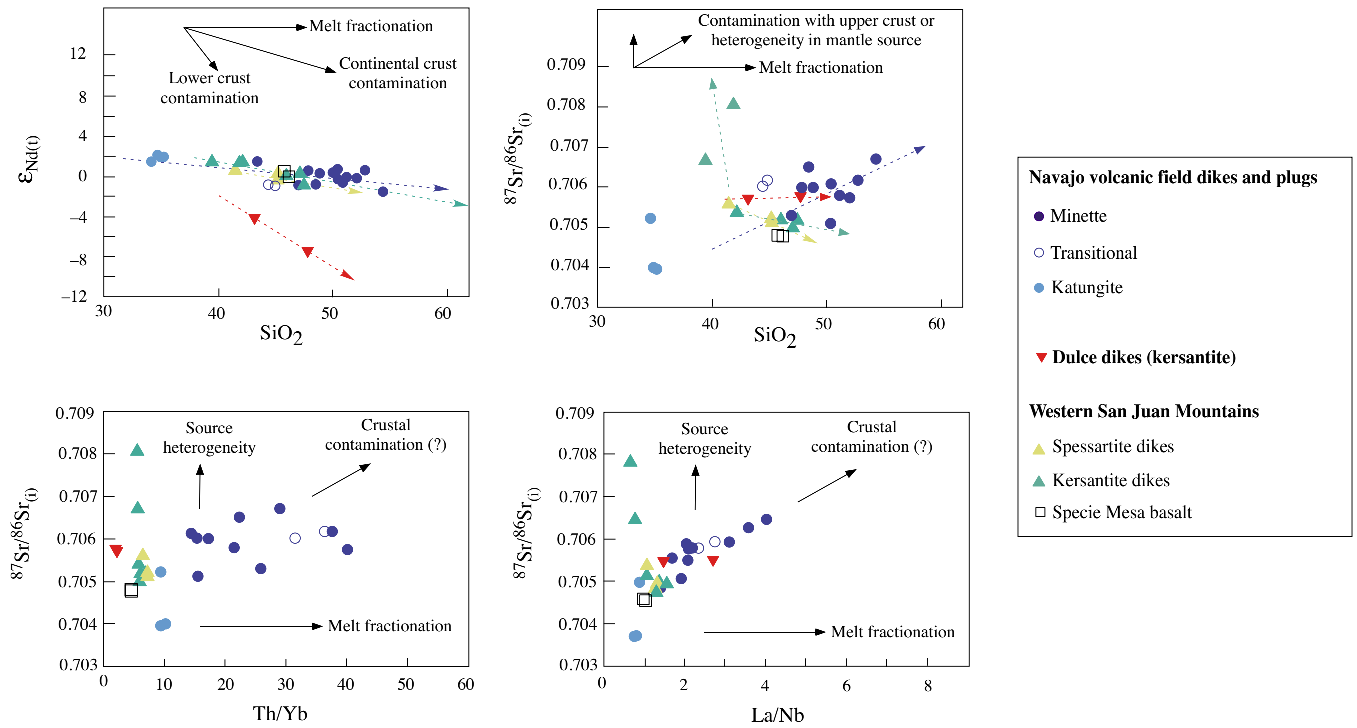

Figure 11. Plots of $\varepsilon_{Nd(t)}$ and $^{87}Sr/^{86}Sr$ against SiO_2 and $^{87}Sr/^{86}Sr$ against Th/Yb and La/Nb for Oligocene to Pleistocene mafic rocks in the Four Corners region. Arrows on the diagrams are drawn to show general trends and do not represent regression lines. The changes in $\varepsilon_{Nd(t)}$ values for Dulce dike rocks could reflect contamination of lithospheric mantle melts by lower crust or melting of a mantle source with low time-integrated Sm/Nd. The variations in $^{87}Sr/^{86}Sr$ with changes in SiO_2 concentrations are more difficult to interpret. The slight increase in $^{87}Sr/^{86}Sr$ with increasing SiO_2 in samples from the Navajo volcanic field is consistent with source heterogeneity ± minor crustal contamination, but the variable trends for rocks from the Western San Juan Mountains do not support crustal contamination. Plots of $^{87}Sr/^{86}Sr_i$ against Th/Yb and La/Nb also reveal that there are no definitive trends indicative of crustal contamination, but some of the trends (variable $^{87}Sr/^{86}Sr_i$ with similar La/Nb and Th/Yb) could indicate source heterogeneity.

OIB field on different plots (Fig. 5). It is argued that asthenospheric mantle with OIB signatures was the source for some post–26 Ma mafic rocks on the southern Colorado Plateau (Group 1 rocks of Alibert et al., 1986), northwestern Colorado (Group 1 rocks of Leat et al., 1988; Gibson et al., 1992; Gibson et al., 1993), and Wasatch Plateau of Utah (Tingey et al., 1991) (Fig. 1). There is no conclusive evidence that the NVF katungites are derivatives from melting of enriched asthenospheric mantle (source of OIB). Compared to average OIB, the katungites have higher overall LILE and LREE and more radiogenic Sr isotopic ratios that plot close to bulk earth (Fig. 9). If the katungites were generated by melting of enriched asthenosphere, then the chemical and isotopic data indicate that the melts likely interacted with the lithospheric mantle to some degree (Fig. 9). The extremely low SiO_2, high MgO, normative mineralogy, and lower overall $^{87}Sr/^{86}Sr$ ratios of these rocks argue that crustal contamination was not the cause of their elevated LILE and LREE relative to oceanic island basalts.

The compositions of other mafic rocks in the region (NVF minette-transitional rocks, Dulce dikes, and WSM dikes and flows) preclude an origin by direct melting of asthenospheric mantle as revealed by elevated LILE and LREE/HREE (Fig. 7), range of Nd and Sr isotopes (Figs. 9 and 11), and arc-like trace-element patterns (Fig. 8). The data are consistent with partial melting of a heterogeneous, metasomatized mantle, similar to alkaline magmas worldwide (Bell and Blenkinsop, 1989). The majority of NVF and WSM samples (Tables 1–3) are similar in composition to Oligocene to Pliocene mafic rocks in northwestern Colorado (Group 2 rocks of Leat et al., 1988; Johnson and Thompson, 1991; Gibson et al., 1993) and mica-bearing alkaline mafic rocks on the Wasatch Plateau (Tingey et al., 1991); these mafic rocks are also interpreted as products of melts from the subcontinental lithospheric mantle.

The Nd and Sr isotopic compositions of the 25–20 Ma Dulce samples are consistent with contamination of melts by lower continental crust. The isotopic

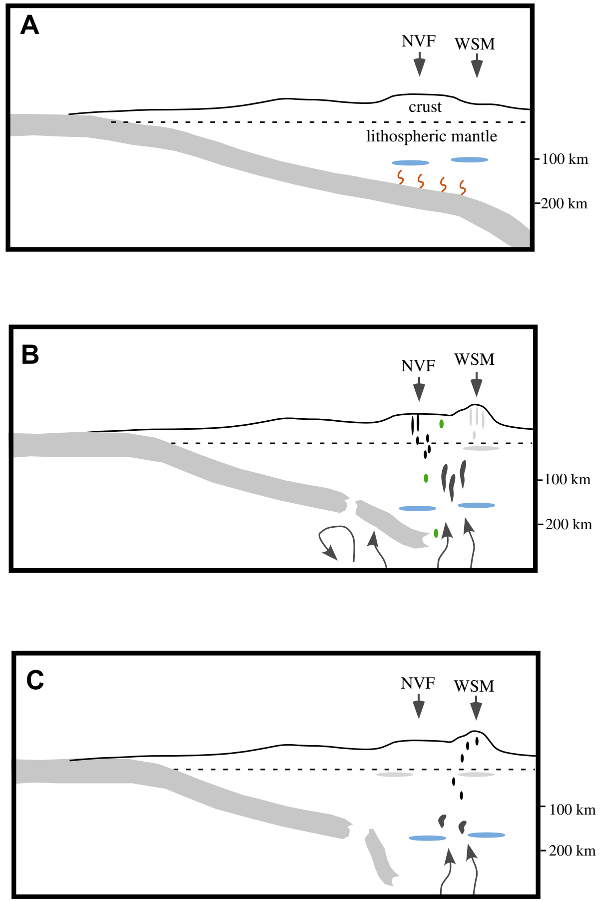

75–30 Ma: The lower 25 to 35 km of the lithosphere is hydrated and "pre-fluxed" by metasomatic fluids (red lines). Heterogeneity in the lithospheric mantle (blue ovals) is likely an artifact created during the assembly of volcanic arcs from 1.8 to 1.7 Ga.

30–20 Ma: Rollback and delamination of the Farallon slab accompanied by incipient extension leads to decompressive-flux melting in the subcontinental lithosphere. Voluminous melting beneath the western San Juan Mountains (WSM) contributed to the production of crustal magmas involved in the ignimbrite flare-up in the Southern Rocky Mountain volcanic field. Melting of the lithospheric mantle, some of which had OIB-like affinities, generated potassic mafic magmas in the Navajo volcanic field (NVF, green ovals). Beneath the Dulce field, mantle melts from the subcontinental lithosphere may have ponded at the crust-mantle boundary and been contaminated with lower crust.

7–0.6 Ma: After the ignimbrite flare-up wanes there is small-volume melting of lithospheric mantle beneath the western San Juan Mountains. This produced alkaline mafic rocks in dike swarms and minor lava flows with distinct chemical traits that may have been caused by the extensive melting and "depletion" of the lithospheric mantle between 29 to 27 Ma or chemical modification of the SCLM during the Proterozoic.

Figure 12. Diagram illustrating the history of magmatic events in the Four Corners region. (A) 75–30 Ma, Laramide subduction and metasomatism of the lithospheric mantle; (B) 30–20 Ma, rollback and delamination of the Laramide slab accompanied by incipient extension in the lithosphere along with emplacement of alkaline mafic magmas during and after the ignimbrite flare-up in the San Juan Mountains; and (C) 7–0.6 Ma, continued emplacement of alkaline mafic magmas on north-northeast zones in the western San Juan Mountains. The 7–0.6 Ma melts were distinguished by distinct chemical traits that could reflect chemical modification of the lithospheric mantle during extensive melting during the Oligocene magmatic events or could be an artifact from the assembly and melting of Proterozoic lithosphere from 1.8 to 1.7 Ga.

signatures of these rocks are similar to Oligocene volcanic rocks in the Southern Rocky Mountain volcanic field (SRMVF on Fig. 1) (e.g., Lipman et al., 1976; Riciputi and Johnson, 1990; Johnson and Thompson, 1991; Riciputi, 1991; Riciputi et al., 1995; Lake, 2013; Lake and Farmer, 2015) that Lake and Farmer (2015) hypothesized were mixtures of mantle magmas with up to 40% mafic lower crust. Alternatively, the Dulce magmas could have formed by partial melting of lithospheric mantle with isotopic affinities similar to those documented for Proterozoic SCLM beneath southern Colorado (Johnson and Thompson, 1991). Leat et al. (1988) also argued that some mafic rocks in northwestern Colorado (Fig. 1) with low $^{143}Nd/^{144}Nd$ ratios (0.5124–0.5119) and near-constant $^{87}Sr/^{86}Sr$ ratios (~0.704) formed by variable contamination of OIB magmas with mafic lower crust (e.g., Kay et al., 1978; Leeman et al., 1985; Dudas et al., 1987) or melting of Proterozoic lithospheric mantle with similar isotopic compositions. The progressive decrease in epsilon Nd values in Dulce rocks from northern New Mexico (–2.6 to –3.3; Gibson et al., 1993) into southern Colorado (–4.2 to –7.5) (Table 3) reveals either variable contamination with lower crustal rocks or regional compositional variations in the SCLM.

The NVF and WSM rocks (minettes and transitional) have similar Nd and Sr isotopic compositions (Fig. 9) but noticeably different concentrations of most major and trace elements (Figs. 4–6; Table 2), revealing a major shift in melt-chemical compositions over time (from 26 to 24 to 7–0.6 Ma). Relative to NVF rocks, those in the WSM are distinguished by lower MgO (Mg#), K_2O, Rb, Zr, La/Lu, La/Ta, La/Nb, and Th/Yb but generally higher Al_2O_3, Na_2O, and CaO. The fact that the Nd and Sr isotopic compositions of NVF and WSM are similar precludes crustal contamination as the cause of the distinct chemical compositions of WSM rocks.

It is argued that 270,000–400,000 km^3 of mafic magma were extracted from the mantle during Oligocene volcanism in the SRMVF (Fig. 1) (Riciputi and Johnson, 1990; Riciputi, 1991; Riciputi et al., 1995; Farmer et al., 2008; Lake and Farmer, 2015). Johnson (1991) concluded that there was a significant contribution of SCLM melts (up to 50%) to the crustal magmas, causing an overall shift to more mafic compositions in the continental crust and local recycling of lower continental crust into the mantle (e.g., Farmer et al., 1991; Hildreth et al., 1991). The extensive melting in this region may have produced a mantle-melt column at least 20–25 km thick (Farmer et al., 2008) in which the more fusible constituents of the SCLM were extracted, leaving it "depleted" in some elements. This idea is supported by experimental melting of phlogopite-bearing lherzolite over 1000° to 1300 °C (Condamine and Médard, 2014): this study is applicable since the SCLM on the eastern edge of the Colorado Plateau contains phlogopite-bearing garnet lherzolite (e.g., McGetchin and Silver, 1970; McGetchin, and Besancon, 1973; Hunter and Smith, 1981; Smith, 1987). Condamine and Médard (2014) demonstrate that higher degrees of melting of phlogopite-bearing mantle could produce potassic melts with increasingly higher MgO (2–12 wt%), FeO (1–7 wt%), and CaO (3–10 wt%) but progressively lower concentrations of Na_2O (5–1 wt%), K_2O (5–3 wt%), and Al_2O_3 (20–14 wt%). This process could leave the mantle source depleted in all of these elements but to different degrees. The differences in major- and trace-element concentrations in the post-7 Ma WSM dike rocks might thus reflect chemical changes in the SCLM as a result of voluminous magma production in the SRVMF from 35 to 26 Ma. Variations in the "fertility" of Proterozoic SCLM from partial melting events from 1.8 to 1.4 Ga could have influenced the higher degrees of melting beneath the WSM (Lee et al., 2001; Gilbert et al., 2007). It is also feasible that lithospheric mantle under the western San Juan Mountains inherited a distinct chemical composition during assembly and alteration of Proterozoic arc terranes as proposed by Gilbert et al. (2007). They concluded that a northeast-trending zone in the lithosphere that extends beneath western Colorado represents a ca. 1.8 Ga subduction-terrane boundary along which ancient mantle rocks were "serpentinized." Alteration of the Proterozoic mantle could have modified the chemical composition of the SCLM in certain zones and may have influenced melt compositions in the late Cenozoic.

Another possible explanation for the differences in chemical composition of NVF and WSM rocks is that a relatively "homogeneous" mantle source with similar isotopic compositions (Fig. 9) underwent different degrees of melting. The melting experiments of Condamine and Médard (2014) produced mafic melts with similar variations in major elements as those in NVF and WSM rocks. In this case, however, it is difficult to reconcile the relatively high Mg# and Ni (and comparable Cr) for NVF rocks, given that they formed by 0.5–1.5% melting of metasomatized SCLM under the Colorado Plateau (e.g., Alibert et al., 1986; Nowell, 1993). The lack of trace-element data for mantle xenoliths on the Colorado Plateau at this time, however, inhibits a test of the idea that different degrees of partial melting caused the distinct compositions of NVF and WSM rocks.

We contend that Oligocene to Pleistocene mafic rocks in the Four Corners region crystallized from magmas that were derived from melting of metasomatized and heterogeneous subcontinental lithospheric mantle enriched in LILE and LREE but with broadly similar Nd and Sr isotopic compositions. The chemical and isotopic data argue that the SCLM beneath the Four Corners region has traits similar to the lithospheric mantle in subduction zones. Navajo volcanic field katungites hint at contributions from the enriched asthenospheric mantle, but this prospect is not clearly supported by the data. The regional SCLM was built by assembly of Proterozoic arcs from 1.8 to 1.4 Ga (e.g., Karlstrom et al., 2005; Gonzales and Van Schmus, 2007) and further modified by Farallon hydration and metasomatism in the Laramide from 75 to 30 Ma (e.g., Smith 1979, 1995; Alibert et al., 1986; Broadhurst, 1986; Roden et al., 1990; Wendlandt et al., 1993, 1996; Usui et al., 2002, 2003; Smith et al., 2004; Smith, 2010; Schulze et al., 2015). Mantle xenoliths in NVF rocks (Smith, 2004) have constrained carbonate-silicate mantle sources of different ages beneath the Colorado Plateau, providing further evidence of the composite magmatic-tectonic history for the regional SCLM. Epsilon Nd values for NVF and WSM rocks lie on the Nd-evolution paths for the most primitive mafic rocks in the Paleoproterozoic complex (Gonzales and Van Schmus, 2007) in southwestern Colorado, consistent with the idea that metasomatized Proterozoic SCLM contributed to the generation of Cenozoic mantle magmas. It is thus conceivable, and reasonable, that the chemical heterogeneity in the subcontinental lithospheric was established during the Proterozoic.

CONCLUSIONS

The different groups of Oligocene to Pleistocene mafic rocks in the Four Corners area (Fig. 2) preserve distinct geochemical variations in both space and time (Figs. 2 and 12). Melt production in any given zone of magmatism (Fig. 2) persisted for 2–7 m.y. and created generations of magmas with broadly similar isotopic and geochemical signatures, reflecting the prolonged similarity in source and process. We argue that chemical variations in the mantle source (SCLM) ± crustal contamination were the dominant influence on the variations in isotopic and geochemical compositions of mafic rocks produced after 26 Ma. The close spatial and temporal relationship of mantle melts emplaced in the region with postcaldera intermediate to felsic plutons from 26 to 3 Ma (Gonzales, 2015) also give insight into the enduring influence of mantle melts on regional trends of crustal magmatism in the transition from convergent tectonics to continental rifting.

Navajo volcanic field rocks were generated by small degrees of melting (<2%) (Nowell, 1993) of SCLM with little or no crustal contamination (revealed by Sr isotopic compositions of cpx crystals; Table 4). The distinct chemical and isotopic signatures of melts generated from 25 to 20 Ma beneath the Dulce field were influenced either by melting of lithospheric mantle with low $^{143}Nd/^{144}Nd$ ratios or mixing of mantle melts with up to 40% lower crustal rocks (Fig. 9). Mafic dikes and flows in the WSM crystallized over ca. 7 Ma from magmas with Nd and Sr isotopic signatures similar to NVF melts but with some distinct differences in major- and trace-element compositions. We argue that the WSM magmas retained a persistent "memory" of chemical modification in the mantle that was influenced by extensive melting (from 35 to 26 Ma) that carried large batches of mafic magmas into the crust. Chemical modification of the lithospheric mantle in this zone could also have been influenced by magmatism and alteration related to subduction processes in the Proterozoic.

Our work contributes to a body of regional research (Fig. 1) that reveals the importance of mantle heterogeneity in the production of alkaline mafic rocks after 26 Ma on the Colorado Plateau (e.g., Alibert, 1994; Alibert et al., 1986; Roden et al., 1990; Tingey et al., 1991; Nowell, 1993; Carlson and Nowell, 2001; Smith et al., 2004; Bailley, 2010) and adjacent Southern Rocky Mountains (e.g., Leat et al., 1988; Johnson and Thompson, 1991; Gibson et al., 1992). It also allows consideration of the role of heterogeneous, ancient subcontinental lithosphere in the production of continental alkaline mafic rocks worldwide.

APPENDIX. ANALYTICAL METHODS AND PARAMETERS

Major- and Trace-Element Analyses

Only unaltered samples or samples with very minor alteration (determined by petrographic analyses) were used for chemical analyses. Whole-rock samples were powdered and analyzed by either Activation Laboratories (methods 4B and 4B2, http://www.actlabs.com/files/Canada_2015.pdf) or SGS Laboratories (http://www.sgs.com). FeO in all samples was determined by the titration method.

SGS Laboratories

Major elements were determined by inductively coupled plasma–atomic emission spectroscopy (ICP-AES) using a lithium-metaborate/tetraborate fusion. Trace elements were determined by inductively coupled plasma–mass spectrometry (ICP-MS) using a sodium peroxide fusion.

In addition to standards analyzed by SGS, internal University of Texas standard (BBB) and a U.S. Geological Survey (USGS) standard (BHVO-2) were analyzed, as well as replicate samples. Compared to mean values of the standards, the SGS values were all within 2-sigma levels of error, and most were within 1-sigma levels.

Activation Laboratories

The following description was taken directly from the Activation Laboratories Web site. Samples for major-element analyses are prepared and analyzed in a batch system. Each batch contains a method reagent blank, certified reference material and 17% replicates.

Prior to sample fusion, the loss on ignition (LOI), which includes H_2O^+, CO_2, S, and other volatiles, was determined from the weight loss after roasting the sample at 1050 °C for 2 h. Samples are mixed with a flux of lithium metaborate and lithium tetraborate and fused in an induction furnace. The molten melt is immediately poured into a solution of 5% nitric acid containing an internal standard and mixed continuously until completely dissolved (~30 min). The samples are run for major oxides and selected trace elements (Code 4B) on a combination simultaneous/sequential Thermo Jarrell-Ash ENVIRO II ICP or a Varian Vista 735 ICP. Calibration is performed using seven prepared USGS and CANMET certified reference materials. One of the seven standards is used during the analysis for every group of ten samples.

For trace-element concentrations, samples fused under code 4B2 are diluted and analyzed by Perkin Elmer Sciex ELAN 6000, 6100, or 9000 ICP/MS. Three blanks and five controls (three before the sample group and two after) are analyzed per group of samples. Duplicates are fused and analyzed every 15 samples. Instrument is recalibrated every 40 samples. Repeated measurements of standards indicate that analytical errors are at the 2 sigma level (95%) (A. Hoffman, Activation Laboratories Ltd., 2016, personal commun.).

Whole-Rock Sr and Nd Isotopic Analyses

(1) Unaltered rock samples and an internal standard from the University of Texas were analyzed for whole-rock Nd and Sr isotopes at the Thermal Ionization Mass Spectrometry Laboratory at the University of Colorado. Samples were dissolved in acid and separated using column chromatography, following the methods of Pin et al. (1994). The $^{87}Sr/^{86}Sr$ ratios were measured using four-collector static mode on a Finnigan-MAT six-collector solid source mass spectrometer.

(2) Total procedural blanks averaged 100 pg for Nd and ~1 ng for Sr.

(3) $^{87}Sr/^{86}Sr$ ratios were measured using the four-collector static mode. The present-day measured $^{87}Sr/^{86}Sr$ ratios were recalculated to determine initial ratios using reported radiometric ages (Gonzales, 2015). Sixteen measurements of SRM-987 for samples analyzed by Lake (2013) yielded a mean value for $^{87}Sr/^{86}Sr$ of 0.71026 ± 0.00002 (2σ), and eight measurements of SRM-987 (Gonzales, this paper) yielded a mean $^{87}Sr/^{86}Sr$ = 0.71028 ± 0.00002 (2σ).

(4) $^{143}Nd/^{144}Nd$ analyses were done in a three-collector dynamic mode. Twelve measurements of the La Jolla Nd standard yielded a mean $^{143}Nd/^{144}Nd$ of 0.511832 ± 8 (2σ). Measured $^{143}Nd/^{144}Nd$ ratios were normalized to $^{146}Nd/^{144}Nd$ = 0.7219.

Sr Isotopic Analyses of Clinopyroxene Single Crystals

(1) All isotopic analyses were performed on a NewWave UP213 LA unit coupled to a NuPlasma HR MC-ICP-MS instrument, housed in the Department of Geological Sciences, University of Cape Town, South Africa. The instrument is a double-focusing ICP-MS fitted with 12 Faraday detectors, three discrete dynode ion counters, and one channeltron ion counter in a fixed-position collector array. Unique variable zoom optics manipulate the ion beam to achieve coincidence and alignment of ion beams of interest. All data were collected on five of the 12 Faraday detectors. Regular Faraday amplifier-gain calibrations ensured relative stability between detectors.

(2) Instrumental mass fractionation was corrected using the exponential law and a fractionation factor based on the measured $^{86}Sr/^{88}Sr$ ratio and the accepted $^{86}Sr/^{88}Sr$ value of 0.1194.

(3) Potential surface contamination was removed by rapidly sweeping the laser along the path of interest (250 mm spot size for analyses, 750 mm line length, 10 Hz repetition rate, 50 μm/s translation rate, 0.25 mJ energy, and 0.5 J/cm2 fluency) prior to the analysis with a narrower beam, higher energy, and slower speed (150–200 mm spot size, 750 mm line length, 20 Hz repetition rate, 5 mm/s translation rate, ±1.35 mJ energy, and ±4.35 J/cm2 fluency).

(4) An in-house standard clinopyroxene (JJG1424 cpx) was analyzed during analyses. Two separate runs generated an average value of 0.7048 ± 0.0004 (n = 15) and 0.7049 ± 0.0001 (n = 4). The accepted value determined for this standard by solution multicollector–inductively coupled plasma–mass spectrometry analysis is 0.70495.

(5) Detailed descriptions of the analytical methods and parameters are provided in Copeland et al. (2008), Radloff et al. (2010), and Le Roux et al. (2014).

ACKNOWLEDGMENTS

We thank the Navajo Division of Natural Resources for providing access to the Navajo Nation to collect samples. A special thanks to Arnold Clifford for helping us navigate to locations in the Navajo volcanic field. We also want to thank Michael Roden, Eric Christiansen, and an anonymous reviewer for their detailed and critical reviews, which improved the quality of this manuscript. This project was funded in part by the National Science Foundation grant 0911290 and several Faculty Development Grants at Fort Lewis College.

REFERENCES CITED

Akers, J.P., Shorty, J.C., and Stevens, P.R., 1971, Hydrogeology of the Cenozoic igneous rocks, Navajo and Hopi Indian Reservations, Arizona, New Mexico, and Utah: U.S. Geological Survey Professional Paper 521-D, 18 p.

Alibert, C., 1994, Peridotite xenoliths from western Grand Canyon and the Thumb: A probe into subcontinental mantle of the Colorado Plateau: Journal of Geophysical Research, v. 99, no. B11, p. 21,605–21,620, doi:10.1029/94JB01555.

Alibert, C., Michard, A., and Albarède, F., 1986, Isotope and trace element geochemistry of Colorado Plateau volcanics: Geochimica et Cosmochimica Acta, v. 50, p. 2735–2750, doi:10.1016/0016-7037(86)90223-1.

Alietti, E., Brigatti, M.F., and Luciano, P., 1995, The crystal structure and chemistry of high-aluminum phlogopite: Mineralogical Magazine, v. 59, p. 149–157, doi:10.1180/minmag.1995.59.394.15.
Appledorn, C.R., and Wright, H.E., 1957, Volcanic structures in the Chuska Mountains, Navajo Reservation, Arizona–New Mexico: Geological Society of America Bulletin, v. 68, p. 445–468, doi:10.1130/0016-7606(1957)68[445:VSITCM]2.0.CO;2.
Bailley, T.L., 2010, A re-evaluation of the origin of Late Cretaceous and younger magmatism in the southern Rocky Mountain region using space-time-composition patterns in volcanic rocks and geochemical studies of mantle xenoliths [Ph.D. thesis]: Boulder, University of Colorado, 152 p.
Bell, K., and Blenkinsop, J., 1989, Neodymium and strontium isotope geochemistry of carbonatites, *in* Bell, K., ed., Carbonatites: Genesis and Evolution: London, Unwin Hyman, p. 278–300.
Bove, D.J., Hon, K., Budding, K.E., Slack, J.F., Snee, L.W., and Yeoman, R.A., 2001, Geochronology and geology of late Oligocene through Miocene volcanism and mineralization in the western San Juan Mountains, Colorado: U.S. Geological Survey Professional Paper 1642, 30 p.
Broadhurst, J.R., 1986, Mineral reactions from xenoliths of the Colorado Plateau: Implications for lower crustal conditions and fluid composition, *in* Dawson, J.B., Carswell, D.A., Hall, J., and Wedepohl, K.H., eds., The Nature of the Lower Continental Crust: Geological Society of London Special Publications 24, p. 331–349, doi:10.1144/GSL.SP.1986.024.01.29.
Bromfield, S.C., 1967, Geology of the Mount Wilson Quadrangle, Western San Juan Mountains, Colorado: U.S. Geological Survey Bulletin 1227, 100 p.
Bush, A.L., Bromfield, C.S., and Pierson, C.T., 1959, Areal geology of the Placerville quadrangle, San Miguel County, Colorado: U.S. Geological Survey Bulletin 1072-E, p. 299–384.
Bush, A.L., Marsh, O.T., and Taylor, R.B., 1960, Areal geology of the Little Cone quadrangle, Colorado: U.S. Geological Survey Bulletin 1802-G, p. 423–492.
Carlson, R.W., and Nowell, G.M., 2001, Olivine-poor sources for mantle-derived magmas: Os and Hf isotopic evidence from potassic magmas of the Colorado Plateau: Geochemistry, Geophysics, Geosystems, v. 2, paper no. 2000GC000128.
Carrara, P.E., 2012, Surficial geologic map of Mesa Verde National Park, Montezuma County, Colorado: U.S. Geological Survey Scientific Investigations Map 3224.
Chapin, C.E., 2012, Origin of the Colorado Mineral Belt: Geosphere, v. 8, p. 28–43, doi:10.1130/GES00694.1.
Chapin, C.E., Wilks, M., and McIntosh, W.C., 2004, Space-time patterns of Late Cretaceous magmatism in New Mexico—Comparison with Andean volcanism and potential for future volcanism: New Mexico Bureau of Geology and Mineral Resources Bulletin, v. 160, p. 13–40.
Condamine, P., and Médard, E., 2014, Experimental melting of phlogopite-bearing mantle at 1 GPa: Implication for potassic magmatism: Earth and Planetary Science Letters, v. 397, p. 80–92, doi:10.1016/j.epsl.2014.04.027.
Condie, K.C., and Selverstone, J., 1999, The crust of the Colorado Plateau: New views of an old arc: The Journal of Geology, v. 107, p. 387–397, doi:10.1086/314363.
Condon, S.M., 1990, Geologic and structure contour map of the Southern Ute Indian Reservation and adjacent areas, Southwest Colorado and Northwest New Mexico: U.S. Geological Survey Miscellaneous Investigations Series, Map I-1958, scale 1:100,000.
Coney, P.J., and Reynolds, S.J., 1977, Flattening of the Farallon slab: Nature, v. 270, p. 403–406, doi:10.1038/270403a0.
Copeland, S.R., Sponheimer, M., le Roux, P.J., Grimes, V., Lee-Thorp, J.A., de Ruiter, D.J., and Richards, M.P., 2008, Strontium isotope ratios ($^{87}Sr/^{86}Sr$) of tooth enamel: A comparison of solution and laser ablation multicollector inductively coupled plasma mass spectrometry methods: Rapid Communications in Mass Spectrometry, v. 22, p. 3187–3194, doi:10.1002/rcm.3717.
Cunningham, C.G., Naeser, C.W., Marvin, R.F., Luedke, R.G., and Wallace, A.R., 1994, Ages of selected intrusive rocks and associated ore deposits in the Colorado Mineral belt: U.S. Geological Survey Bulletin 2109, 31 p.
Deer, W.A., Howie, R.A., and Zussman, J., 1978, An introduction to the rock-forming minerals: London, Longman Group Limited, 328 p.
Dudas, F.O., Carlson, R.W., and Eggler, D.H., 1987, Regional middle Proterozoic enrichment of the subcontinental mantle sources of igneous rocks from central Montana: Geology, v. 15, p. 22–25, doi:10.1130/0091-7613(1987)15<22:RMPEOT>2.0.CO;2.
Dungan, M.A., Lindstrom, M.E., McMillan, N.J., Moorbath, S., Hoefs, J., and Haskin, L.A., 1986, Open system magmatic evolution of the Taos Plateau volcanic field, northern New Mexico 1: The petrology and geochemistry of the Servilleta Basalt: Journal of Geophysical Research, v. 91, p. 5999–6028, doi:10.1029/JB091iB06p05999.
Ehrenberg, S.N., 1979, Garnetiferous ultramafic inclusions in minette from the Navajo volcanic field, *in* Boyd, F.R. and Meyer, H.O.A., eds., The Mantle Sample: Inclusions in Kimberlites and Other Volcanics: Washington, D.C., American Geophysical Union, Proceedings of the Second International Kimberlite Conference, v. 2, p. 330–344.
Esperanca, S., and Holloway, J.R., 1987, On the origin of some mica-lamprophyres: Experimental evidence from a mafic minette: Contributions to Mineralogy and Petrology, v. 95, p. 207–216, doi:10.1007/BF00381270.
Farmer, G.L., Broxton, D.E., Warren, R.G., and Pickthorn, W., 1991, Nd, Sr, and O isotopic variations in metaluminous ash-flow tuffs and related volcanic rocks at the Timber Mountain/Oasis Valley Caldera, Complex, SW Nevada: Implications for the origin and evolution of large-volume silicic magma bodies: Contributions to Mineralogy and Petrology, v. 109, no. 1, p. 53–68, doi:10.1007/BF00687200.
Farmer, G.L., Bailley, T., and Elkins-Tanton, L.T., 2008, Mantle source volumes and the origin of the mid-Tertiary ignimbrite flare-up in the southern Rocky Mountains, western U.S: Lithos, v. 102, no. 1–2, p. 279–294, doi:10.1016/j.lithos.2007.08.014.
Fitton. J.G., James, D., Kempton, P.D., Ormerod, D.S., and Leeman, W.P., 1988, The role of lithospheric mantle in the generation of Late Cenozoic basaltic magmas in the western United States: Journal of Petrology, Special Lithosphere Issue, p. 331–349, doi:10.1093/petrology/Special_Volume.1.331.
Fitton, J.G., James, D., and Leeman, W.P., 1991, Basic magmatism associated with late Cenozoic extension in the western United States: Compositional variations in space and time: Journal of Geophysical Research, v. 96, no. B8, p. 13,693–13,711, doi:10.1029/91JB00372.
Gartner, A.E., and Delaney, P.T., 1988, Geologic map showing a late Cenozoic basaltic intrusive complex, Emery, Sevier, and Wayne counties, Utah: U.S. Geological Survey Map MF-2052, 1 sheet.
Gibson, S.A., Thompson, R.N., Leat, P.T., Dickin, A.P., Morrison, M.A., Hendry, G.L., and Mitchell, J.G., 1992, Asthenosphere-derived magmatism in the Rio Grande rift, western USA: Implications for continental break-up, *in* Storey, B.C., Alabaster, T., and Pankhurst, R.J., eds., Magmatism and the Causes of Continental Break Up: Geological Society of London Special Publications 68, p. 61–89, doi:10.1144/GSL.SP.1992.068.01.05.
Gibson, S.A., Thompson, R.N., Leat, P.T., Dickin, A.P., Morrison, M.A., Hendry, G.L., Dickin, A.P., and Mitchell, J.G., 1993, Ultrapotassic along the flanks of the Oligo-Miocene Rio Grande Rift, USA: Monitors of the zone of lithospheric mantle extension and thinning beneath a continental rift: Journal of Petrology, v. 34, no. part 1, p. 187–228, doi:10.1093/petrology/34.1.187.
Gibson, S.A., Thompson, R.N., Dickin, A.P., and Leonardos, O.H., 1995, High-Ti and low-Ti mafic potassic magmas: Key to plume lithosphere interactions and continental flood-basalt genesis: Earth and Planetary Science Letters, v. 136, p. 149–165, doi:10.1016/0012-821X(95)00179-G.
Gilbert, H., Velasco, A.A., and Zandt, G., 2007, Preservation of Proterozoic terrane boundaries within the Colorado Plateau and implications for its tectonic evolution: Earth and Planetary Science Letters, v. 258, p. 237–248, doi:10.1016/j.epsl.2007.03.034.
Gonzales, D.A., 2009, Insight into Middle Tertiary crustal extension and mantle magmatism along the northern margin of the San Juan Basin at the onset of volcanism in the San Juan Mountains: Geological Society of America Abstracts with Programs, v. 41, no. 6, p. 32, paper no. 10-4.
Gonzales, D.A., 2013, New age constraints on middle to late Cenozoic plutons in the western San Juan Mountains, southwestern Colorado: Implications for landscape evolution: Geological Society of America Abstracts with Programs, v. 45, no. 5, p. 3, paper no. 2-6.
Gonzales, D.A., 2015, New U/Pb zircon and $^{40}Ar/^{39}Ar$ age constraints of the Cenozoic plutonic record, southwestern Colorado: Implications for regional magmatic-tectonic evolution: The Mountain Geologist, v. 52, no. 2, p. 5–32.
Gonzales, D.A., and Van Schmus, W.R., 2007, Proterozoic history and crustal evolution in Southwestern Colorado: Insight from U/Pb and Sm/Nd data: Precambrian Research, v. 154, no. 1–2, p. 31–70, doi:10.1016/j.precamres.2006.12.001.
Gonzales, D.A., Turner, B.E., Burgess, R.T., Holnback, C.C., and Critchley, M.R., 2010, New insight into the timing and history of diatreme-dike complexes of the northeastern Navajo Volcanic Field, southwestern Colorado, *in* Fassett, J.E., Zeigler, K., and Lueth, V.W., eds., Geology of

the Four Corners Country: New Mexico Geological Society, 60th Field Conference Guidebook, p. 163–172.

Gregory, H.E., 1917, Geology of the Navajo country: A reconnaissance of parts of Arizona, New Mexico, and Utah: U.S. Geological Survey Professional Paper 93, 161 p.

Hildreth, W., Halliday, A.N., and Christiansen, R.L., 1991, Isotopic and chemical evidence concerning the genesis and contamination of basaltic and rhyolitic magma beneath the Yellowstone Plateau volcanic field: Journal of Petrology, v. 32, p. 63–138, doi:10.1093/petrology/32.1.63.

Humphreys, E., Hessler, E., Dueker, K., Farmer, G.L., Erslev, E., and Atwater, T., 2003, How Laramide-age hydration of North American lithosphere by the Farallon slab controlled subsequent activity in the western United States: International Geology Review, v. 45, issue 7, p. 575–595.

Humphreys, E.D., 1995, Post-Laramide removal of the Farallon slab, western United States: Geology, v. 23, p. 987–990, doi:10.1130/0091-7613(1995)023<0987:PLROTF>2.3.CO;2.

Hunter, W., and Smith, D., 1981, Garnet peridotite from Colorado Plateau ultramafic diatremes: Hydrates, carbonates, and comparable geothermometry: Contributions to Mineralogy and Petrology, v. 76, p. 312–320, doi:10.1007/BF00375458.

Johnson, C.M., 1991, Large-scale crust formation and lithosphere modification beneath middle to late Cenozoic calderas and volcanic fields, western North America: Journal of Geophysical Research, v. 96, p. 13,485–13,507, doi:10.1029/91JB00304.

Johnson, C.M., and Thompson, R.A., 1991, Isotopic composition of Oligocene mafic volcanic rocks in the northern Rio Grande rift: Evidence of contributions of ancient intraplate and subduction magmatism to evolution of the lithosphere: Journal of Geophysical Research, v. 96, p. 13,593–13,608, doi:10.1029/91JB00342.

Johnson, C.M., Lipman, P.W., and Czamanske, G.K., 1990, H, O, Sr, Nd, and Pb isotope geochemistry of the Latir volcanic field and cogenetic intrusions, New Mexico, and relations between evolution of a continental magmatic center and modification of the lithosphere: Contributions to Mineralogy and Petrology, v. 104, p. 99–124, doi:10.1007/BF00310649.

Karlstrom, K.E., Whitmeyer, S.J., Dueker, K., Williams, M.L., Bowring, S.A., Levander, A., Humphreys, E.D., and Keller, G.R., and the CD-ROM Working Group, 2005, Synthesis of results from the CD-ROM experiment: 4-D image of the lithosphere beneath the Rocky Mountains and implications for understanding the evolution of continental lithosphere, *in* Karlstrom, K.E., and Keller, G.R., eds., The Rocky Mountain Region: An Evolving Lithosphere (Tectonics, Geochemistry, and Geophysics): American Geophysical Union Geophysical Monograph Series 154, p. 421–441, doi:10.1029/154GM31.

Kay, S.M., Kay, R.W., Hangus, J., and Snedden, T., 1978, Crustal xenoliths from potassic lavas, Leucite Hills, Wyoming: Geological Society of America Abstracts with Programs, v. 3, p. 432.

Kheirkhah, M., Neill, I., and Allen, M.B., 2015, Petrogenesis of OIB-like basaltic rocks in a continental collision zone: Late Cenozoic magmatism of eastern Iran: Journal of Asian Earth Sciences, v. 106, p. 19–33, doi:10.1016/j.jseaes.2015.02.027.

Lake, E.T., 2013, Geochemical and thermal insights into caldera-forming “super-eruptions” [Ph.D. thesis]: The University of Texas at Austin, available online: http://catalog.lib.utexas.edu/record=b8307669~S29.

Lake, E.T., and Farmer, G.L., 2015, Oligo-Miocene mafic intrusions of the San Juan Volcanic Field, southwestern Colorado, and their relationship to voluminous, caldera-forming magmas: Geochimica et Cosmochimica Acta, v. 157, p. 86–108, doi:10.1016/j.gca.2015.02.020.

Laughlin, A.W., Aldrich, M.J., Shafiqullah, M., and Husler, J., 1986, Tectonic implications of the age, composition, and orientation of the lamprophyre dikes, Navajo volcanic field, Arizona: Earth and Planetary Science Letters, v. 76, p. 361–374, doi:10.1016/0012-821X(86)90087-7.

Leat, P.T., Thompson, R.N., Morrison, M.A., Hendry, G.L., and Dickin, A.P., 1988, Compositionally-diverse Miocene–Recent rift-related magmatism in northwest Colorado: Partial melting, and mixing of mafic magmas from 3 different asthenospheric and lithospheric mantle sources: Journal of Petrology, Special Lithosphere Issue, p. 351–377.

Le Bas, M.J., Le Maitre, R.W., Streckeisen, A., and Zanettin, B., 1986, A chemical classification of volcanic rocks based on the total alkali-silica diagram: Journal of Petrology, v. 27, p. 745–750, doi:10.1093/petrology/27.3.745.

Lee, C.-T., Yin, Q., Rudnick, R.L., and Jacobsen, S.B., 2001, Preservation of ancient and fertile lithospheric mantle beneath the southwestern United States: Nature, v. 411, p. 69–73, doi:10.1038/35075048.

Leeman, W.P., Menzies, M.A., Matty, D.J., and Embee, G.F., 1985, Strontium, neodymium, and lead composition of deep crustal xenoliths from the Snake River Plain: Evidence for Archean basement: Earth and Planetary Science Letters, v. 75, no. 4, p. 354–368, doi:10.1016/0012-821X(85)90179-7.

Le Maitre, R.W., Bateman, P., Dudek, A., Keller, J., Lameyre, J., Le Bas, M.J., Sabine, P.A., Schmid, R., Sorensen, H., Streckeisen, A., Woolley, A.R., and Zanettin, B., 1989, A Classification of Igneous Rocks and Glossary of Terms: Recommendations of the International Union of Geological Sciences Subcommission on the Systematics of Igneous Rocks: Oxford, UK, Blackwell Scientific Publications, 193 p.

Le Roux, P.J., Lee-Thorp, J.A., Copeland, S.R., Sponheimer, M., and de Ruiter, D.J., 2014, Strontium isotope analysis of curved tooth enamel surfaces by laser-ablation multi-collector ICP-MS: Palaeogeography, Palaeoclimatology, Palaeoecology, v. 416, p. 142–149, doi:10.1016/j.palaeo.2014.09.007.

Lipman, P.W., compiler, 1989, International Association of Volcanology and Chemistry of the Earth’s Interior (IAVCEI) field trip guide: Oligocene–Miocene San Juan volcanic field, Colorado: New Mexico Bureau of Mines and Mineral Resources Memoir, v. 46, p. 303–380.

Lipman, P.W., 2006, Geologic map of the central San Juan cluster, southwestern Colorado: U.S. Geological Survey Geologic Investigation Series I-2799, map and pamphlet.

Lipman, P.W., 2007, Incremental assembly and prolonged consolidation of Cordilleran magma chambers: Evidence from the Southern Rocky Mountain volcanic field: Geosphere, v. 3, p. 42–70, doi:10.1130/GES00061.1.

Lipman, P.W., and Zimmerer, M.J., 2016, Magmato-tectonic links: Ignimbrite calderas, regional dike swarms, and the transition from arc to rift in the southern Rocky Mountains: Geological Society of America Abstracts with Programs, v. 48, no. 7, paper 54-9, doi:10.1130/abs/2016AM-278823.

Lipman, P.W., Fisher, F.S., Mehnert, H.H., Naeser, C.W., Luedke, R.G., and Steven, T.A., 1976, Multiple ages of mid-Tertiary mineralization and alteration in the western San Juan Mountains, Colorado: Economic Geology and the Bulletin of the Society of Economic Geologists, v. 71, p. 571–588, doi:10.2113/gsecongeo.71.3.571.

Lipman, P.W., Doe, B.R., Hedge, C.E., and Steven, T.A., 1978, Petrologic evolution of the San Juan volcanic field, southwestern Colorado: Pb and Sr isotope evidence: Geological Society of America Bulletin, v. 89, p. 59–82, doi:10.1130/0016-7606(1978)89<59:PEOTSJ>2.0.CO;2.

Lloyd, F.E., Arima, M., and Edgar, A.D., 1985, Partial melting of a phlogopite-clinopyroxenite nodule from southwest Uganda: An experimental study bearing on the origin of highly potassic continental rift volcanics: Contributions to Mineralogy and Petrology, v. 91, p. 321–329, doi:10.1007/BF00374688.

McDonough, W.F., 1990, Constraints on the composition of the continental lithospheric mantle: Earth and Planetary Science Letters, v. 101, p. 1–18.

McGetchin, T.R., and Besancon, J., 1973, Carbonate inclusions in mantle-derived pyropes: Earth and Planetary Science Letters, v. 18, p. 408–410, doi:10.1016/0012-821X(73)90096-4.

McGetchin, T.R., and Silver, L.T., 1970, Compositional relations in minerals from kimberlite and related rocks in the Moses Rock dike, San Juan County, Utah: The American Mineralogist, v. 55, p. 1738–1771.

Menzies, M.A., Arculus, R.J., Best, M.G., Bergman, S.C., Ehrenberg, S.N., Irving, A.J., Roden, M.F., and Schulze, D.J., 1987, A record of subduction processes and within-plate volcanism in lithospheric xenoliths of the southwestern USA, *in* Nixon, P.H., ed., Mantle Xenoliths: New Jersey, John Wiley and Sons Ltd., p. 59–74.

Mitchell, R.H., 1995, Kimberlites, orangeites and related rocks: New York, Plenum Press, 410 p., doi:10.1007/978-1-4615-1993-5.

Mitchell, R.H., 1997, Kimberlites, orangeites, lamproites, melilitites and minettes: A petrographic atlas: Thunder Bay, Canada, Almaz Press, Inc., 243 p.

Naeser, C.W., 1971, Geochemistry of the Navajo-Hopi diatremes: Journal of Geophysical Research, v. 76, p. 4978–4985, doi:10.1029/JB076i020p04978.

Nowell, G.M., 1993, Cenozoic potassic magmatism and uplift of the western United States [Ph.D. thesis]: Milton Keynes, UK, Open University, 251 p.

Nybo, J.P., 2014, ^{40}Ar/^{39}Ar geochronology of the Navajo volcanic field [M.S. thesis]: Socorro, New Mexico, New Mexico Institute of Mining and Technology Department of Earth and Environmental Science, 137 p.

Nybo, J.P., McIntosh, W.C., and Semken, S.C., 2011, Ar-Ar phlogopite geochronology of the Navajo volcanic field and the Ship Rock diatreme of northwest New Mexico define a 1.4 Ma

pulse of potassic magmatism: American Geophysical Union Conference, December 2011, abstract V23A-2566.
Pearce, J.A., 1983, Role of the sub-continental lithosphere on magma genesis at active continental margins, *in* Hawkesworth, C.J., and Norry, M.J., eds., Continental Basalts and Mantle Xenoliths: Nantwich, Cheshire, Shiva Publications, p. 230–249.
Pearce, J.A., and Peate, D.W., 1995, Tectonic implications of the composition of volcanic arc magmas: Annual Reviews of Earth and Planetary Sciences, v. 23, p. 251–285.
Peccerillo, R., and Taylor, S.R., 1976, Geochemistry of Eocene calc-alkaline volcanic rocks from the Kastamonu area, northern Turkey: Contributions to Mineralogy and Petrology, v. 58, p. 63–81, doi:10.1007/BF00384745.
Pin, C., Briot, D., Bassin, C., and Poitrasson, F., 1994, Concomitant separation of strontium and samarium-neodymium for isotopic analysis in silicate samples, based on specific extraction chromatography: Analytica Chimica Acta, v. 298, p. 209–217, doi:10.1016/0003-2670(94)00274-6.
Radloff, F.G.T., Mucina, L., Bond, W.J., Le Roux, P.J., 2010, Strontium isotope analyses of larger herbivore habitat use in the Cape Fynbos region of South Africa: Oecologia, v. 164, p. 567–578.
Riciputi, L.R., 1991, Petrology and Nd, Sr, and Pb isotopes of the central San Juan caldera cluster, Colorado [Ph.D. thesis]: University of Wisconsin, Madison.
Riciputi, L.R., and Johnson, C.M., 1990, Nd and Pb-isotope variations in the multicycle central caldera cluster of the San Juan volcanic field, Colorado, and implications for crustal hybridization: Geology, v. 18, p. 975–978, doi:10.1130/0091-7613(1990)018<0975:NAPIVI>2.3.CO;2.
Riciputi, L.R., Johnson, C.M., Sawyer, D.A., and Lipman, P.W., 1995, Crustal and magmatic evolution in a large multicycle caldera complex: Isotopic evidence from the central San Juan volcanic field: Journal of Volcanology and Geothermal Research, v. 67, p. 1–28, doi:10.1016/0377-0273(94)00097-Z.
Righter, K., and Rosas-Elguera, J., 2001, Alkaline lava in the volcanic front of the western Mexican volcanic belt: Geology and petrology of the Ayulta and Tapalpa volcanic fields: The Journal of Geology, v. 42, no. 12, p. 2333–2361.
Riter, J.C.A., 1999, Geochemical and tectonic evolution of the Colorado Plateau mantle lithosphere: Evidence from Grand Canyon mantle xenoliths [Ph.D. thesis]: The University of Texas at Austin, 261 p.
Riter, J.C.A., and Smith, D., 1996, Xenolith constraints on the thermal history of the mantle below the Colorado Plateau: Geology, v. 24, no. 3, p. 267–270, doi:10.1130/0091-7613(1996)024<0267:XCOTTH>2.3.CO;2.
Rock, N.M.S., 1977, The nature and origin of lamprophyres: Some definitions, distinctions, and derivations: Earth-Science Reviews, v. 13, p. 123–169, doi:10.1016/0012-8252(77)90020-4.
Rock, N.M.S., 1991, Lamprophyres: Glasgow, UK, Blackie, p. 125–149.
Roden, M.F., Smith, D., and McDowell, F.W., 1979, Age and extent of potassic volcanism on the Colorado Plateau: Earth and Planetary Science Letters, v. 43, p. 279–284, doi:10.1016/0012-821X(79)90212-7.
Roden, M.F., Smith, D., and Murthy, V.M., 1990, Chemical constraints on lithosphere composition and evolution beneath the Colorado Plateau: Journal of Geophysical Research, v. 95, no. B3, p. 2811–2831, doi:10.1029/JB095iB03p02811.
Roden, M.F., and Smith, D., 1979, Field geology, chemistry, and petrology of Buell Park minette diatreme, Apache County, Arizona, *in* Boyd, F.R., and Meyer, H.O.A., eds., The Mantle Sample: Inclusions in Kimberlites and Other Volcanics: American Geophysical Union Proceedings of the Second International Kimberlite Conference, v. 2, p. 364–381.
Rollinson, H., 1993, Using geochemical data: Evaluation, presentation, interpretation: Essex, England, Longman Scientific and Technical, 352 p.
Rudnick, R.L., McDonough, W.F., and Chappell, B.W., 1993, Carbonatite metasomatism in the northern Tanzanian mantle: Petrographic and geochemical characteristics: Earth and Planetary Science Letters, v. 114, p. 463–475, doi:10.1016/0012-821X(93)90076-L.
Schulze, D.J., Davis, D.W., Helmstaedt, H., and Joy, B., 2015, Timing of the Cenozoic "Great Hydration" event beneath the Colorado Plateau: Th-Pb dating of monazite in the Navajo volcanic field metamorphic eclogite xenoliths: Geology, v. 43, no. 8, p. 727–730, doi:10.1130/G36932.1.
Sekine, T., and Wyllie, P.J., 1983, Experimental simulation of mantle hybridization in subduction zones: The Journal of Geology, v. 91, p. 511–528, doi:10.1086/628802.
Slack, J.F., and Lipman, P.W., 1979, Chronology of alteration, mineralization, and caldera evolution in the Lake City area, western San Juan Mountains, Colorado, *in* Ridge, J.D., ed., Papers on Mineral Deposits of Western North America: Snowbird, Utah, Fifth International Association on the Genesis of Ore Deposits (IAGOD) Symposium, Nevada Bureau of Mines Geology Report 33, p. 151–158.
Smith, D., 1979, The Mantle Sample: Inclusion in Kimberlites and Other Volcanics, *in* Boyd, F.R., and Meyer, H.O.A., eds., The Mantle Sample: Inclusion in Kimberlites and Other Volcanics: Washington, D.C., American Geophysical Union, p. 345–356, doi:10.1029/SP016p0345.
Smith, D., 1987, Genesis of carbonate in pyrope form ultramafic diatremes on the Colorado Plateau, southwestern United States: Contributions to Mineralogy and Petrology, v. 97, p. 389–396, doi:10.1007/BF00372001.
Smith, D., 1995, Chlorite-rich ultramafic reaction zones in Colorado plateau xenoliths: Recorders of sub-Moho hydration: Contributions to Mineralogy and Petrology, v. 121, p. 185–200, doi:10.1007/s004100050098.
Smith, D., 2010, Antigorite peridotite, metaserpentinite, and other inclusions within diatremes on the Colorado Plateau, SW USA: Implications for the mantle wedge during low-angle subduction: Journal of Petrology, v. 51, p. 1355–1379, doi:10.1093/petrology/egq022.
Smith, D., Griffin, W.L., Ryan, C.G., and Soey, S.H., 1991, Trace-element zonation in garnets from the Thumb: Heating and melt infiltration below the Colorado Plateau: Contributions to Mineralogy and Petrology, v. 107, p. 60–79, doi:10.1007/BF00311185.
Smith, D., Connelly, J.N., Manser, K., Moser, D.E., Housh, T.B., McDowell, F.W., and Mack, L.E., 2004, Evolution of Navajo eclogites and hydration of the mantle wedge below the Colorado Plateau, southwestern United States: Geochemistry, Geophysics, Geosystems, v. 5, no. 4, Q04005, doi:10.1029/2003GC000675.
Smith, G.A., 2004, Middle to Late Cenozoic developments of the Rio Grande rift and adjacent regions in northern New Mexico, *in* Mack, G.H., and Giles, K.A., eds., The Geology of New Mexico: New Mexico Geological Society Special Publication 11, p. 331–358.
Spera, F.J., and Bohrson, W.A., 2001, Energy-constrained open-system magmatic processes I: General model and energy-constrained assimilation and fractional crystallization (EC-AFC) formulation: Journal of Petrology, v. 42, no. 5, p. 999–1018, doi:10.1093/petrology/42.5.999.
Steckeisen, A., 1979, A classification and nomenclature of volcanic rocks, lamprophyres and melilitic rock: Recommendations and suggestions of the IUGS Subcommision of the Systematics of Igneous Rocks: Geology, v. 7, p. 331–335.
Steven, T.A., Lipman, P.W., and Hail, W.J., Barker, Fred, and Luedke, R.G., 1974, Geologic map of the Durango quadrangle, southwestern Colorado: U.S. Geological Survey, Miscellaneous Investigations Series Map I-764, scale 1:250,000.
Sun, S.S., and McDonough, W.F., 1989, Chemical and isotopic systematics of oceanic basalts: Implications for mantle composition and processes, *in* Saunders, A.D., and Norry, M.J., eds., Magmatism in Ocean Basins: Geologic Society of London Special Publications 42, p. 313–345, doi:10.1144/GSL.SP.1989.042.01.19.
Taylor, S.R., and McLennan, S.M., 1985, The continental crust: Its composition and evolution: Boston, Blackwell Scientific, 312 p.
Thompson, R.N., Gibson, S.A., Leat, P.T., Morrison, M.A., Hendry, G.L., Dickin, A.P., and Mitchell, J.G., 1993, Early–Miocene continental extension-related magmatism at Walton Peak, northwest Colorado: Further evidence on continental basalts genesis: Journal of the Geological Society of London, v. 150, p. 277–292, doi:10.1144/gsjgs.150.2.0277.
Tingey, D.G., Christiansen, E.H., Best, M.G., Ruiz, R., and Lux, D.R., 1991, Tertiary minette and melanephelinite dikes, Wasatch Plateau, Utah: Records of mantle heterogeneities and changing tectonics: Journal of Geophysical Research, v. 96, no. B8, p. 13,529–13,544, doi:10.1029/91JB00327.
Tweto, O., 1980, Tectonic history of Colorado, *in* Kent, H.C., and Porter, K.W., ed., Colorado Geology: Denver, Colorado, Rocky Mountain Association of Geologists, p. 5–9.
Tweto, O., and Sims, P.K., 1963, Precambrian ancestry of the Colorado mineral belt: Geological Society of America Bulletin, v. 74, p. 991–1014, doi:10.1130/0016-7606(1963)74[991:PAOTCM]2.0.CO;2.
Usui, T., Kobayashi, K., and Nakamura, E., 2002, U-Pb isotope systematics of micro-zircon inclusions: Implications for the age and origin of eclogite xenoliths from the Colorado Plateau: Proceedings of the Japan Academy, Ser. B., v. 78, p. 51–56.
Usui, T., Nakamura, E., Kobayashi, K., Maruyama, S., and Helmstaedt, H., 2003, Fate of the subducted Farallon plate inferred from eclogite xenoliths in the Colorado Plateau: Geology, v. 31, p. 589–592, doi:10.1130/0091-7613(2003)031<0589:FOTSFP>2.0.CO;2.
Wallace, P., and Carmichael, I.S.E., 1989, Minette lavas and associated leucitites from Western Front of the Mexican volcanic belt: Petrology, chemistry, and origin: Contributions to Mineralogy and Petrology, v. 103, p. 470–492, doi:10.1007/BF01041754.

Wareham, C.D., 1991, Isotopic and geochemical studies of a Pliocene porphyry-Mo system, Rico, Colorado [Ph.D. thesis]: Aberdeen, Scotland, Aberdeen University, 288 p.
Wareham, C.D., Rice, C.M., Boyce, A.J., and Rogers, G., 1998, S, C, Sr, and Pb sources in the Pliocene Silver Creek porphyry Mo system, Rico, Colorado: Economic Geology and the Bulletin of the Society of Economic Geologists, v. 93, p. 32–46, doi:10.2113/gsecongeo.93.1.32.
Warner, L.A., 1980, The Colorado lineament, *in* Kent, H.C. and Porter, K.W., eds., Colorado Geology: Denver, Colorado, Rocky Mountain Association of Geologists, p. 11–21.
Wendlandt, E., DePaulo, D.J., and Baldridge, W.S., 1993, Nd and Sr isotope chronostratigraphy of Colorado Plateau lithosphere: Implications for magmatic and tectonic underplating of the continental crust: Earth and Planetary Science Letters, v. 116, p. 23–43, doi:10.1016/0012-821X(93)90043-9.
Wendlandt, E., DePaulo, D.J., and Baldridge, W.S., 1996, Thermal history of Colorado Plateau lithosphere from Sm-Nd geochronology of xenoliths: Geological Society of America Bulletin, v. 108, no. 7, p. 757–767, doi:10.1130/0016-7606(1996)108<0757:THOCPL>2.3.CO;2.
Williams, H., 1936, Pliocene volcanoes of the Navajo-Hopi country: Geological Society of America Bulletin, v. 47, p. 111–172, doi:10.1130/GSAB-47-111.
Wood, G.H., Kelley, V.C., and MacAlpin, A.J., 1948, Geology of the southern part of Archuleta Country, Colorado: U.S. Geological Survey, Oil and Gas Investigations Map OM-81, scale 1:63,360.
Woolley, A.R., Bergman, S.C., Edgar, A.D., Le Bas, M.J., Mitchell, R.H., Rock, N.M.S., and Scott Smith, B.H., 1996, Classification of lamprophyres, lamproites, kimberlites, and the kalsilitic, melilitic, and leucitic rocks: Journal of The Mineralogical Association of Canada, v. 34, no. 2, p. 175–186.
Wyllie, P.J., and Sekine, T., 1982, The formation of mantle phlogopite in subduction zone hybridization: Contributions to Mineralogy and Petrology, v. 79, p. 375–380, doi:10.1007/BF01132067.
Zindler, A., and Hart, S., 1986, Chemical geodynamics: Annual Review of Earth and Planetary Science Letters, v. 14, p. 493–571, doi:10.1146/annurev.ea.14.050186.002425.